

University of Alberta

**STABILITY AND BIFURCATION ANALYSIS ON
DELAY DIFFERENTIAL EQUATIONS**

by

Xihui Lin

A thesis submitted to the Faculty of Graduate Studies and Research
in partial fulfillment of the requirements for the degree of

Master of Science

in

Applied Mathematics

Department of Mathematical and Statistical Sciences

© Xihui Lin

Fall 2012

Edmonton, Alberta

Permission is hereby granted to the University of Alberta Libraries to reproduce single copies of this thesis and to lend or sell such copies for private, scholarly, or scientific research purposes only. Where the thesis is converted to, or otherwise made available in digital form, the University of Alberta will advise potential users of the thesis of these terms.

The author reserves all other publication and other rights in association with the copyright in the thesis and, except as herein before provided, neither the thesis nor any substantial portion thereof may be printed or otherwise reproduced in any material form whatsoever without the author's prior written permission.

Abstract

Most recent studies on delay differential equations are mainly focused on local stability analysis, stability switches, and local existence of Hopf bifurcations with only one delay included, while the global existence of Hopf bifurcation and stability analysis with two delays are hardly discussed. In this thesis, we numerically explore global behaviors of Hopf branches arising from where the characteristic roots crossing the imaginary axis, and we reveal that there seems to be a strong and simple underlying rule, which is been partly studied by Li and Shu in their recent paper [Li & Shu 2010a]. In addition, stability analysis on delay differential equations with two discrete delays will also be studied. We extend the work by [Gu *et al.* 2005], and establish a similar theory on a more general type of models. Finally, we provide some preliminary results for the two-delay models with parameters depending on one delay.

Acknowledgements

This thesis work is mainly under the instruction of Dr. Hao Wang and Dr. Michael Li, from whom the initial guess of global behaviors of Hopf branches originates. I would like to thank them for their creative ideas and thoughtful suggestions. During my stay in University of Alberta, Dr. Hao Wang motivated and helped me a lot. All these are greatly appreciated. I also would like to thank Dr. Hongying Shu for her nice work on global Hopf bifurcation [Li & Shu 2010b] and her helpful discussion.

Table of Contents

1	An introduction to delay differential equations	1
1.A	Definition of delay differential equations	2
1.B	Definition of stability	6
1.C	Linearization and characteristic equations	8
1.D	Hopf bifurcation	11
1.E	Floquet multiplier and stability of periodic solution	14
2	Stability and bifurcation analysis of DDEs with one delay	16
2.A	A geometric stability switch criteria	17
2.B	Introduction to DDE-BIFTOOL: a MATLAB package for bifurcation analysis of DDEs	20
2.C	Global Hopf bifurcation with delay independent parameters: HTLV-I infection with CTL response	21
2.C.1	Model Of HTLV-I infection with CTL response	21
2.C.2	Stability analysis	22
2.C.3	Stability switch and global Hopf bifurcation case I: $G(u)$ has two positive roots	28
2.C.4	Stability switch and global Hopf bifurcation case II: $G(u)$ has three positive roots	31

2.C.5	Summary and discussion on the HTLV-I infection model	36
2.D	Global Hopf bifurcation with delay dependent parameters : de- layed Lotka-Volterra model	39
2.D.1	Delayed Lotka-Volterra model	39
2.D.2	Stability of the boundary equilibrium P_1	42
2.D.3	Stability of the coexistence equilibrium P_2	44
2.D.4	Model with Holling Type I functional response: stability and global Hopf bifurcation	47
2.D.5	Model with Holling Type II functional response: stabil- ity and global Hopf bifurcation	51
2.D.6	Discussion	57
3	Stability analysis of delay differential equations with two de- lays	59
3.A	Stability crossing curves of models with delay independent pa- rameters	61
3.A.1	Stability crossing curves	62
3.A.2	Crossing direction	67
3.B	Stability crossing curves of models with parameters depending on one delay	70
3.C	An example: a population model with inner competition	71
4	Discussion and future work	76
	Bibliography	78

List of Figures

2.1	Transfer diagram of CTL response to HTLV-I infection.	21
2.2	Graph of $G(u)$ with two positive roots.	29
2.3	Bifurcation diagram showing stability switches at P_2 and global Hopf branches bifurcating from those switches τ values. Parameters are given as follows: $\lambda = 160$, $\beta = 0.002$, $\gamma = 0.2$, $\mu = 0.2$, $d_1 = 0.16$, $d_2 = 1.845$, $d_3 = 0.5$	30
2.4	Periodic solution on the 2nd Hopf branches in the overlap stable interval in Figure 2.3, with $\tau = 69.4$. Period of this solution is about 61.1.	31
2.5	Periodic solution on the 3rd Hopf branches in the overlap stable interval in Figure 2.3, with $\tau = 69.4$. Period of this solution is about 34.2.	32
2.6	Floquet multipliers for periodic solutions around secondary bifurcation points on the second branch (left) and the third branch (right) as shown in Figure 2.3	33
2.7	Graph of $G(u)$ with three positive roots.	33

2.8	Bifurcation diagram showing stability switch at P_2 and the global Hopf branches, with parameters given in (2.19). Solid lines indicate stable branches, and dashed lines indicate unstable branches.	34
2.9	Two stable periodic solutions for the same set of parameters and same delay $\tau = 5$	35
2.10	Four periodic solutions for $\tau = 12, \tau = 15, \tau = 23, \tau = 100$ showing the period-doubling effect.	37
2.11	Projection of the periodic solution in Figure 7 with $\tau = 100$ to the xyz -space and its power spectrum from FFT.	37
2.12	Graph of $S_n(\tau)$. We see that only S_0, S_1, S_2 have zeros.	49
2.13	Global Hopf bifurcation.	50
2.14	Two stable periodic solutions for $\tau = 70$, which lies in the overlap of the stable intervals in Figure 2.13.	50
2.15	Left: periods of periodic solutions on the overlap stable region. Right: norm of the nontrivial Floquet multipliers with largest norm on the overlap stable region.	51
2.16	Graph of $S_n(\tau)$. We see that only S_0, S_1 have zeros.	55
2.17	Global Hopf bifurcation.	55
2.18	Two stable periodic solutions for $\tau = 73.5$, which lies in the overlap of the stable intervals in Figure 2.17.	56

2.19	Torus bifurcations on the lower branch shown in 2.17 as a pair of complex Floquet multipliers cross the unit circle. Left: A pair of Floquet multipliers at the first secondary bifurcation point move inside the unit circle; Right: A pair of Floquet multipliers at the second secondary bifurcation point move outside the unit circle.	56
2.20	Left: periods of periodic solutions on the overlap stable region. Right: norm of the nontrivial Floquet multipliers with largest norm on the overlap stable region.	57
3.1	Zero contour of $g(\omega, \tau)$ with parameters given in (3.37), with which $\tau_m = 5.3648$	74
3.2	Stability crossing curves. The index n increases along the arrow.	75

Chapter 1

An introduction to delay differential equations

In many applications, when using ordinary differential equations or partial differential equations, one always assumes that a system is governed by the principle of causality, namely, the future state of the system is determined by the current state only while the past has no impact on the future with the present of the current state. However, this is not logically reasonable in many processes in biology, medicine, economics, chemistry etc. For example, in epidemic model, the person who gets a virus infection usually does not immediately show symptom or become infectious until a certain latency ends. As a matter of fact, the principle of causality is only a first approximation to the reality and a more realistic model should also take into account the impact of the past state. This is the motivation of the theory on delay differential equations.

In this chapter, we first give a formal definition of delay differential equations and some of their basic properties, parallel to the theory of ordinary

differential equations. Linearization and characteristic equations as the main technique on local stability of equilibria is introduced in section 3. In section 4, we describe the Hopf bifurcation theorem on delay differential equations, which is one of the main theorems used through the whole thesis. Finally, Floquet's theory on periodic solutions forms the main topic of section 5.

1.A Definition of delay differential equations

Before giving a definition of delay differential equations, we need to declare some notations. Through this thesis, we use \mathbb{R}^n to denote an n -dimensional real Euclidean space. For $a < b$, we denote $C([a, b], \mathbb{R}^n)$ the Banach space of all continuous functions mapping the interval $[a, b]$ into \mathbb{R}^n with the topology of uniform convergence, i.e, $\|\phi\| = \sup_{a \leq \theta \leq b} |\phi(\theta)|$, if $\phi \in C([a, b], \mathbb{R}^n)$. We use *sup* here instead of *max* to allow the possibility of $a = -\infty$. If $[a, b] = [-r, 0]$, where r is a positive constant, we simply denote $C = C([-r, 0], \mathbb{R}^n)$.

Definition: For $\sigma \in \mathbb{R}$, $A \geq 0$, $t \in [\sigma, \sigma + A]$, $x \in C([\sigma - r, \sigma + A], \mathbb{R}^n)$, we define $x_t \in C$ as $x_t(\theta) = x(t + \theta)$, $\theta \in [-r, 0]$. If Ω is a subset of $\mathbb{R} \times C$, $f : \Omega \rightarrow \mathbb{R}^n$ is a given function, and $'$ represents the right-hand derivative, we call

$$x'(t) = f(t, x_t) \tag{1.1}$$

a retarded functional differential equation (RFDE) or a delay differential equation (DDE) on Ω .

A function x is called a *solution* of Equation (1.1) on $[\sigma - r, \sigma + A]$ if there are $\sigma \in \mathbb{R}$ and $A > 0$, such that $x \in C([\sigma - r, \sigma + A], \mathbb{R}^n)$, $(t, x_t) \in \Omega$ and

$x(t)$ satisfies Equation (1.1) for $t \in [\sigma, \sigma + A]$. For given $\sigma \in \mathbb{R}$, $\phi \in C$, we say $x_t(\sigma, \phi, f)$ is a *solution* of Equation (1.1) with initial value ϕ at σ or simply a *solution* through (σ, ϕ) if there is an $A > 0$ such that $x_t(\sigma, \phi, f)$ is a solution of Equation (1.1) on $[\sigma - r, \sigma + A]$ and $x_\sigma(\sigma, \phi, f) = \phi$. If the solution is unique, then for each $t \geq 0$, we can define the solution map of the initial problem of (1.1) as

$$T(t) : \phi \rightarrow x_t(\sigma, \phi). \quad (1.2)$$

Obviously $T(t)$ maps C to C .

Equation (1.1) is said to be *linear* if $f(t, x_t) = L(t, x_t) + h(t)$, where $L(t, x_t)$ is linear with respect to x_t . If $f(t, x_t) = g(x_t)$, which is independent of t , we say Equation (1.1) is autonomous; otherwise, we say (1.1) is nonautonomous. For an autonomous DDE, the solution map T defined in (1.2) does not depend on t , and can be proved that under this point of view, x_t as a solution of Equation (1.1) forms a semi-flow on the metric space C , whose dimension is infinity. This makes the complexity of DDEs, as compared to ODEs. We will see more when coming to the characteristic equations.

As a matter of fact, the definition of DDEs here is very general, including ODEs (if $r = 0$), ODEs, and some integro-differential equations. Here are some of the examples.

$$\begin{aligned} x'(t) &= f(x(t), x(t - \tau_1), \dots, x(t - \tau_p)), \quad t \geq 0, \\ x_0 &= \phi, \end{aligned} \quad (1.3)$$

where $0 < \tau_1 < \tau_2 < \dots < \tau_p = r$;

$$x'(t) = \int_{-r}^0 g(t, s, x(t + s)) ds. \quad (1.4)$$

In applications, we choose to model with an autonomous DDE as we think that the *laws of nature* which hold now are identical to those for any point in the past or future. In addition, DDEs with discrete time independent delays are preferred for mathematical convenience. Here in this thesis, we mainly focus on this type of DDEs with constant delays, i.e., Equations (1.3). However even for this simple version, there is not a very efficient way to analyze the dynamics.

Some basic theories on existence, and uniqueness, continuous dependence, forward continuation are shown and proved in [Hale & Verduyn Lunel 1993], [Smith 2011]. Here we only list those results.

Theorem 1.1 (Existence): *In (1.1), suppose Ω is an open subset in $\mathbb{R} \times C$, and f is continuous on Ω . If $(\sigma, \phi) \in \Omega$, then there is a solution of (1.1) passing through (σ, ϕ) .*

Theorem 1.2 (Uniqueness): *Suppose Ω is an open set in $\mathbb{R} \times C$, f is continuous on Ω , and $f(t, \phi)$ is Lipschitz in ϕ for any compact set $K \subset \Omega$, i.e., for any $(t, \phi_1), (t, \phi_2) \in K$, there exists a constant $k > 0$, such that*

$$|f(t, \phi_1) - f(t, \phi_2)| \leq k|\phi_1 - \phi_2|.$$

If $(\sigma, \phi) \in \Omega$, then there is a unique solution of Equation (1.1) through (σ, ϕ) .

Theorem 1.3 (Continuous dependence): *Suppose Ω is an open set in $\mathbb{R} \times C$, f is continuous on Ω , and x is a solution of Equation (1.1) through (σ, ϕ) , which exists and is unique on $[\sigma - r, b]$, $b > \sigma - r$. Let $W \subseteq \Omega$ be the compact*

set defined by

$$W = \{(t, x_t) : t \in [\sigma, b]\},$$

and let V be a neighborhood of W on which f is bounded. if (σ^k, ϕ^k, f^k) , $k = 1, 2, \dots$, satisfies $\sigma^k \rightarrow \sigma$, $\phi^k \rightarrow \phi$, and $|f^k - f|_V \rightarrow 0$ as $k \rightarrow \infty$, then there is a K such that, for $k \geq K$, each solution $x^k = x^k(\sigma^k, \phi^k, f^k)$ through (σ^k, ϕ^k) of

$$\frac{dx(t)}{dt} = f^k(t, x_t)$$

exists on $[\sigma^k - r, b]$ and $x^k \rightarrow x$ uniformly on $[\sigma - r, b]$. Since some x^k may not be defined on $[\sigma - r, b]$, by $x^k \rightarrow x$ uniformly on $[\sigma - r, b]$, we mean that for any $\epsilon > 0$, there is a $k_1(\epsilon)$ such that $x(t)$, $k \geq k_1(\epsilon)$, is defined on $[\sigma - r + \epsilon, b]$ and $x^k \rightarrow x$ uniformly on $[\sigma - r + \epsilon, b]$.

Theorem 1.4 (Forward continuation): *Suppose Ω is an open set in $\mathbb{R} \times C$, f is completely continuous on Ω , and x is a noncontinuable solution of Equation (1.1) on $[\sigma - r, b)$. Then for any closed bounded set $U \subset \Omega$, there is a t_U such that $(t, x_t) \notin U$ for $t_U \leq t < b$.*

In other words, the theorem above says that solution of Equation (1.1) either exists for all $t \geq \sigma$ or becomes unbounded (with respect to Ω) at some finite time. For backward continuation, more conditions are needed, which can be seen from the following theorem.

Theorem 1.5 (Smoothing property): *Let $x(t)$ be the solution of*

$$x'(t) = f(t, x_t), \quad x_\sigma = \phi, \quad \phi \in C, \quad (1.5)$$

where $f \in C^k$, $k \geq 1$, i.e, f has continuous k^{th} derivative, and $I = [\sigma, t_x)$

the maximum interval of existence for $x(t)$. Then $x(t) \in C^l$ on $[\sigma + lr, t_x)$ for $l = 0, 1, \dots, k$.

In other words, the solution $x(t)$ gains smoothness up to C^k as time goes. Therefore if the initial function $\phi \notin C^1$, backward continuation is impossible. Furthermore, the initial data ϕ should satisfy $\phi'(\sigma) = f(\sigma, \phi_\sigma)$, where $\phi'(\sigma)$ denotes the left-derivative. Therefore, in order to extend the solution backwards, the initial data ϕ should be very special in C . In deed, we will need some very technical condition sufficient condition to ensure the possibility of backward continuation, which is shown in Theorem 5.1 of [Hale & Verduyn Lunel 1993]. To the contrary, for ODEs, forward and backward continuation have no difference, and the solution $x(t)$ is C^k when $f(t, x)$ is C^k wherever it exists.

Theorem 1.6 (Positivity of autonomous DDEs with constant delays): *In Equation (1.3), suppose $f(x, y_1, \dots, y_p)$ and $f_x(x, y_1, \dots, y_p)$ are continuous, and for any $i = 1, 2, \dots, n$, $t \geq 0$, $x, y_1, \dots, y_p \in \mathbb{R}_+^n$, we always have*

$$f_i(x, y_1, \dots, y_p) \geq 0, \text{ if } x_i = 0.$$

Then given a positive initial data ϕ , the corresponding solution $x(t)$ of (1.3) is also positive wherever it exists.

1.B Definition of stability

Assume $\sigma = 0$, and for any given initial data in C , solution exists for $t \geq 0$. Considering the system (1.1), a solution $y(t)$ is called *stable* if for any $\varepsilon > 0$, there exists $\delta > 0$, such that $\phi \in C$ and $\|\phi - y_0\| < \delta$ implies $\|x_t - y_t\| < \varepsilon$ for

$t \geq 0$. It is *asymptotically stable* if $\|x_t(\phi) - y_t\| \rightarrow 0$ as $t \rightarrow +\infty$. It is *unstable* if it is not stable.

A solution $x(t)$ of (1.1) is called an *equilibrium* if $x_t = x_0$ for all t , i.e., $x(t + \theta) = x(\theta)$ for any $t \geq 0$, $-r \leq \theta \leq 0$. Thus $x(t)$, as an equilibrium of (1.1) should be a constant function. Therefore, to obtain all the equilibria of a DDE, we only need to solve

$$f(t, x^*) = 0, \forall t \geq 0 \tag{1.6}$$

for x^* .

A solution $x(t)$ of (1.1) is called a *periodic solution* if there exists a $T > 0$, such that $x(t + T) = x(t)$ for all $t \geq 0$. T is then call the period of $y(t)$. Stability assertions of a periodic solution can not be asymptotically stable from the definition above, because $y(t) = x(t + \theta)$ is also a periodic solution, and if $\theta \neq 0$ is small, $\|x_0 - y_0\|$ is also small, while $\|x(t) - y(t)\| \not\rightarrow 0$ as $t \rightarrow \infty$. Instead, we define stability of periodic solution in the orbital sense. We say a periodic solution $x(t)$ is (*orbitally*) *stable* if for every $\varepsilon > 0$ there exists $\delta > 0$ such that if $d(y_0, O(x_0)) < \delta$, then $d(y_t, O(x_0)) < \varepsilon$ for all $t \geq 0$. Here $O(x_0) = \{x_t : t \in R_+\} \subset C$ is called the *orbit* of x_0 , and $d(y_0, O(x_0)) = \inf\{\|y_0 - \phi\| : \phi \in O(x_0)\}$ denotes the distance between the point y_0 and the subset $O(x_0)$ in C .

These two kinds of special solutions, equilibria and periodic solutions, along with their stability are of our main interests in this thesis.

1.C Linearization and characteristic equations

Consider a homogeneous linear autonomous delay system

$$x'(t) = Ax + \sum_{i=1}^p B_i x(t - \tau_i) \quad (1.7)$$

We see that $x = 0$ is an equilibrium, and it is the only equilibrium if $A + \sum_{i=1}^p B_i$ is non-singular. By the theory of dynamical system, we know that all solutions of (1.7) are (asymptotically) stable if and only if $x = 0$ is (asymptotically) stable.

Same logic as what we do with ODEs, we seek exponential solutions of (1.7) of the form

$$x(t) = He^{\lambda t}, \quad H \neq 0,$$

where $\lambda \in \mathbb{C}$ and $H \in \mathbb{C}^n$. We plug it into (1.7) and get

$$\lambda e^{\lambda t} H = e^{\lambda t} A + e^{\lambda t} H \left(\sum_{i=1}^p e^{-\lambda \tau_i} B_i \right),$$

\implies

$$(\lambda I - A - \sum_{i=1}^p e^{-\lambda \tau_i} B_i) H = 0. \quad (1.8)$$

(1.8) has non-zero solution if and only if

$$D(\lambda) := \det(\lambda I - A - \sum_{i=1}^p e^{-\lambda \tau_i} B_i) = 0. \quad (1.9)$$

We call $D(\lambda)$ the characteristic function of (1.7), and its roots are said to be characteristics or eigenvalues of (1.7).

The following theorems show some important properties of the character-

istic function [Smith 2011].

Theorem 1.7: (Properties of the characteristic equation)

- (i) $D(\lambda)$ is an entire function;
- (ii) If λ is a characteristic root, so is $\bar{\lambda}$;
- (iii) Given $\sigma \in \mathbb{R}$, there are at most finitely many characteristic roots in $\lambda \in \mathbb{C} : \text{Re}\lambda > \sigma$;
- (iv) If there are infinitely many distinct characteristic roots $\{\lambda_n\}$, then

$$\text{Re}\lambda_n \rightarrow -\infty, n \rightarrow \infty.$$

Theorem 1.8: Suppose $\text{Re}\lambda < \mu$ for every characteristic root λ . Then there exists $K > 0$, such that

$$|x(t, \phi)| < Ke^{\mu t} \|\phi\|, t \geq 0, \phi \in C, \quad (1.10)$$

where $x(t, \phi)$ is the solution of (1.7) with initial condition $x_0 = \phi$. so the equilibrium $x = 0$ of (1.7) is asymptotically stable if all the characteristic roots have negative real parts. On the other hand, if there exists a root with positive real part, it is unstable.

From the above theorem, to study stability of the linear dynamical system (1.7), one needs only to verify if there exists a characteristic root with positive real part. Fortunately, by Theorem 1.7, these roots are at most finitely many. Our main goal left in this chapter is find these roots.

Before we move on to our main goal, we need to know how we can use these results of the linear system to study general autonomous DDEs.

Consider the nonlinear autonomous delay differential equation with constant delays

$$x'(t) = f(x_t) := f(x(t), x(t - \tau_1), \dots, x(t - \tau_p)), \quad (1.11)$$

where $f \in C^1(\mathbb{R}^{(p+1) \times n})$.

Suppose x^* is a steady state or equilibrium of (1.11), i.e., $f(x^*) = 0$. If $x(t)$ is a solution of (1.11), let $u(t) = x(t) - x^*$. Then $u(t)$ satisfies

$$u'(t) = f(x^* + u_t). \quad (1.12)$$

To study the stability of x^* , we need to track the behavior of solution of (1.11) near x^* , i.e., the behavior of solution of (1.12) near $u(t) = 0$. For this purpose, we expand the right hand side as a Taylor series to the first degree

$$u'(t) = Df(x^*, \dots, x^*)(u(t)^T, u(t - \tau_1)^T, \dots, u(t - \tau_p)^T)^T + o(\|u(t)\|),$$

where T denotes transpose of a matrix, and $Df(x^*, \dots, x^*)$ is value of the Jacobi matrix of f at $(x^{*T}, \dots, x^{*T})^T$. The constant term $f(x^*, \dots, x^*)$ is ignored as it is zero. We call

$$u'(t) = Df(x^*, \dots, x^*)(u(t)^T, u(t - \tau_1)^T, \dots, u(t - \tau_p)^T)^T \quad (1.13)$$

the *linearized system or equation* of (1.11) about x^* .

The following theorem reveals the relation of system (1.11) and its linearized system (1.13).

Theorem 1.9 (Local stability of nonlinear autonomous DDEs): *Let $D(\lambda)$ be the characteristic equation corresponding to (1.13), then x^* is locally asymptotically stable if every root of $D(\lambda)$ has negative real part. In fact, there exist $\delta > 0$, $K > 0$ such that*

$$\|\phi - x^*\| < \delta \implies \|x_t(\phi) - x^*\| \leq K \|\phi - x^*\| e^{-\mu t}, \quad t \geq 0$$

where

$$-\mu := \sup_{D(\lambda)=0} \operatorname{Re} \lambda < 0.$$

On the other hand, x^ is unstable if one of the roots of $D(\lambda)$ has positive real part.*

1.D Hopf bifurcation

One significant problem of applying a mathematical model to simulate and predict the future state of a real process is that we need to know the value of parameters introduced in the model. Although we may have some real data from observation and could use them to estimate our parameters, the exact value cannot be assured since errors usually accompany with observations. In fact, there may not be a true value for each parameter because there are usually complex and unpredictable small perturbations in the real world and data we get are just some samples which may be different if obtained even in a completely same circumstance. Furthermore an efficient numerical method may not be available to estimate some of the parameters. In some cases, the variation of a parameter has no significant impact on the dynamics, while in other cases, it may change the dynamics completely. Therefore we have to

analyze the system with all the possible values of parameters of our interest. In the thesis, we focus on the time delays, which play a crucial role in delayed systems as it usually brings up oscillation as compared to ODE models. Among all the bifurcation phenomena, Hopf bifurcation is the most important one as it companies with a periodic solution. In this section, we give a description of the Hopf bifurcation theorem.

Consider the following delay differential equation with one parameter,

$$x'(t) = F(x_t, \alpha). \quad (1.14)$$

where $F \in C^2(C \times \mathbb{R})$, and α is a scale parameter.

Without loss of generality, we assume $x = 0$ is an equilibrium for all value of α , i.e., $F(0, \alpha) \equiv 0$. Suppose that the linearized equation of (1.14) is

$$u'(t) = L(\mu)u_t \quad (1.15)$$

where $L(\mu) : C \rightarrow \mathbb{R}^n$ is a linear operator. Let $D(\lambda, \alpha)$ be the associated characteristic function and $\lambda_{1,2}(\alpha) = \mu(\alpha) \pm i\omega(\alpha)$ are one pair of the roots. We make following two assumptions on these characteristic roots.

(H1) For $\alpha = 0$, $\lambda_{1,2}(0) = \pm i\omega_0$ are simple roots and no other roots that is a integer multiple of $i\omega_0$.

(H2) $\mu'(0) \neq 0$.

The first assumption implies that $\mu(0) = 0$, $\omega(0) = \omega_0$ and $D_\lambda(0, i\omega_0) \neq 0$.

Therefore by the implicit function theorem, both functions $\mu(\alpha)$, $\omega(\alpha)$ are differentiable. The second assumption is to ensure that this pair of complex roots will cross the imaginary axis to other side as α increases through 0.

The Hopf theorem describes below is mainly taken from [Smith 2011]. Its proof can be found in many books on nonlinear dynamics.

Theorem 1.10: *Suppose that assumption (H1) and (H2) hold. Then there exists $\varepsilon > 0$, real-valued even functions $\alpha(\varepsilon)$ and $T(\varepsilon) > 0$ satisfying $\alpha(0) = 0$ and $T(0) = 2\pi/\omega_0$, and a non-constant $T(\varepsilon)$ -periodic function $p(t, \varepsilon)$ with all functions being continuously differentiable in ε for $|\varepsilon| < \varepsilon_0$, such that $p(t, \varepsilon)$ is a solution of (1.14) and $p(t, \varepsilon) = \varepsilon q(t, \varepsilon)$ where $q(t, 0)$ is a $2\pi/\omega_0$ -periodic solution of $q' = L(0)q$.*

Moreover, there exist $\alpha_0, \beta_0, \delta_0 > 0$ such that if (1.14) has a nonconstant periodic solution $x(t)$ of period P for some α satisfying $|\alpha| < \alpha_0$ with $\max_t |x(t)| < \beta_0$ and $|P - 2\pi/\omega_0| < \delta$, then $\alpha = \alpha(\varepsilon)$ and $x(t) = p(t + \theta, \varepsilon)$ for some $|\varepsilon| < \varepsilon_0$ and some θ .

If $F \in C^5(C \times \mathbb{R}^n)$, then

$$\begin{aligned}\alpha(\varepsilon) &= \alpha_1 \varepsilon^2 + O(\varepsilon^4) \\ T(\varepsilon) &= \frac{2\pi}{\omega_0} [1 + \tau_1 \varepsilon^2 + O(\varepsilon^4)]\end{aligned}$$

If all other characteristic roots for $\alpha = 0$ have strictly negative real parts except for $\pm i\omega_0$, then $p(t, \varepsilon)$ is asymptotically stable if $\alpha_1 \mu' > 0$ and unstable if $\alpha_1 \mu' < 0$.

The phenomenon this theorem describes is called *Hopf bifurcation*. It mainly tells us that under some smooth conditions, when there are a pair of simple conjugate characteristic roots across the imaginary axis to the other side of the complex plane, a unique periodic solution appears in the neighborhood of the equilibrium when the bifurcation parameter α is close enough to the bifurcation point $\alpha = 0$.

1.E Floquet multiplier and stability of periodic solution

Consider the nonlinear functional differential equation with discrete delays (1.11). Suppose that $p(t)$ is periodic solution of (1.11) with period T . To study the stability, we again linearize the system about this periodic solution. Let $x(t) = p(t) + u(t)$, then

$$\begin{aligned} u'(t) &= f(p_t + u_t) - p'(t) = f(p_t + u_t) - f(p_t) \\ &= Df(p_t)u_t + o(\|u_t\|), \quad 0 \leq t \leq T, \end{aligned}$$

where $Df(p_t) = Df(p(t), p(t-\tau_1), \dots, p(t-\tau_p))$ is the Jacobi matrix of $f(x, y_1, y_2, \dots, y_p)$ at $p(t)$.

Denote $A(t) := Df(p_t)$. It is obvious that $A(t)$ is of T -period. We call

$$u'(t) = A(t)u_t \tag{1.16}$$

the linearized system of (1.11) about $p(t)$. We define a map in C as below,

$$S_T : \phi \rightarrow u(T, \phi).$$

Obviously, S_T is linear and bounded as $A(t)$ is linear and bounded. We call the eigenvalues of S_T *Floquet multipliers* of (1.11) with respect to the periodic solution $p(t)$. We denote as $FL(p)$ to be all Floquet multipliers with respect to $p(t)$. If there is a $\mu \in \mathbb{C}$ such that $e^{\mu T}$ is a Floquet multiplier, then we say μ is a Floquet exponent. Notice that Floquet exponents are not unique as $e^{(\mu+2\pi ki/T)T} = e^{\mu T}$, $k \in \mathbb{Z}$. However, the real parts are unique and are called Lyapunov exponents.

The following theorem reveals the relationship between a nonlinear system and its correspondent linearized system about a periodic solution.

Theorem 1.11 (Floquet multipliers): *Assume $p(t)$ to be a T -periodic solution of (1.11), and (1.16) is the corresponding linearized system about $p(t)$, then*

- (i) $1 \in FL(p)$ (we call it the trivial Floquet multiplier) ;
- (ii) $p(t)$ is (orbital) stable if 1 is a single eigenvalue and all non-trivial Floquet multipliers lies inside the unit circle on the complex plane, i.e.,

$$|\lambda| < 1, \forall \lambda \in FL(p) \setminus \{1\};$$

To the contrary, $p(t)$ is (orbital) unstable if there is a non-trivial Floquet multipliers lies outside the unit circle on the complex plane.

Chapter 2

Stability and bifurcation

analysis of DDEs with one delay

Models with one constant delay are the simplest and most common delayed models in mathematical biology. Although it is the simplest, analyzing stability of equilibria is still quite technical, especially when parameters are delay dependent. Characteristic equations of delayed models are transcendental and analytical or numerical methods on this kind of equations are not well developed at the present. In this chapter, we first introduce a method proposed by Beretta and Kuang[Beretta & Kuang 2002] to find critical delay values where stability switches and Hopf bifurcation occur. In section 2, we give a brief description on the MATLAB package DDE-BIFTOOL which we use throughout this thesis to analyze global behaviors of Hopf branches. In section 3 and section 4, we apply these methods to the HTLV-I infection model with CTL response and the classical delayed Lotka-Volterra predator prey model.

2.A A geometric stability switch criteria

In this section we study the occurrence of any possible stability switch as the value of the time delay τ increases with a general characteristic equation of the form

$$D(\lambda, \tau) := P_n(\lambda, \tau) + Q_m(\lambda, \tau)e^{-\lambda\tau} = 0, \quad (2.1)$$

where $n, m \in \mathbb{N}_0$, $n > m$, $\tau \in I := [0, \tau_m)$ and

$$P_n(\lambda, \tau) = \sum_{j=0}^n p_j(\tau)\lambda^j, \quad Q_m(\lambda, \tau) = \sum_{j=0}^m q_j(\tau)\lambda^j, \quad (2.2)$$

both of which are analytic function of λ and differentiable in τ . In the section, we assume the followings:

- (i) $\lambda = 0$ is not a root of $D(\lambda, \tau)$, i.e., $P_n(0, \tau) + Q_m(0, \tau) = p_0(\tau) + q_0(\tau) \neq 0$;
- (ii) $\limsup\{|Q_m(\lambda, \tau)|/|P_n(\lambda, \tau)|: |\lambda| \rightarrow \infty, \operatorname{Re} \lambda > 0\} < 1, \forall \tau > 0$;
- (iii) $F(\omega, \tau) := |P_n(i\omega, \tau)|^2 - |Q_m(i\omega, \tau)|^2$ is not a zero polynomial for each τ ;
- (iv) Each positive zero $\omega(\tau)$ of $F(\omega, \tau)$ is continuous and differentiable in τ wherever it exists.

Assumption (i) is to exclude fold bifurcation and make sure any root crossing the imaginary axis can result in a Hopf bifurcation. Assumption (ii) is to ensure that there are not points bifurcating from infinity. Assumption (iii) is to guarantee there are only finite "gates" for roots to cross the imaginary axis and assumption (iv) is to ensure that we can take derivative of $\omega(\tau)$.

To study stability switch, i.e., to obtain bifurcation values, we need to track

the signs of all characteristic roots as τ increases from 0 to wherever it exists. The basic idea is to first find all the roots of $D(\lambda, \tau)$ when $\tau = 0$, which is a polynomial whose roots are easy to compute. Next, we seek critical values of τ , said τ^* where there are roots $\lambda(\tau)$ crossing the imaginary axis, i.e., there are pure imaginary characteristic roots. If $\left. \frac{d\text{Re } \lambda}{d\tau} \right|_{\tau=\tau^*} > 0$, we know that this characteristic root will cross the imaginary axis to the right and there will be one more characteristic root with positive real part. On the other hand, if $\left. \frac{d\text{Re } \lambda}{d\tau} \right|_{\tau=\tau^*} < 0$, then we know that this characteristic root will cross the imaginary axis to the left and the number of characteristic roots with positive real parts are reduced by 1. For both situations, a Hopf bifurcation occurs and periodic solution appears. Furthermore, if we know the number of characteristic roots with positive real parts when $\tau = 0$ (DDE then becomes ODE), then we know the number of characteristic roots with positive real parts over the whole τ interval, and stability of the steady state are completely understood.

Assume $\lambda = i\omega$ ($\omega > 0$) is a characteristic root, then $-i\omega$ is also a characteristic root since $D(\lambda, \tau)$ is a real function. Thus we have

$$|P_n(i\omega, \tau)| = |Q_m(i\omega, \tau)e^{-i\omega\tau}| = |Q_m(i\omega, \tau)|.$$

Hence $F(\omega, \tau) = |P_n(i\omega, \tau)|^2 - |Q_m(i\omega, \tau)|^2 = 0$. It is clear that $F(\omega, \tau)$ is a polynomial for each given τ , and therefore all the positive roots are relatively easy to compute. Denote $\omega(\tau)$ to be any of them. To solve $D(i\omega(\tau), \tau) = 0$ for τ is equivalent to solve

$$e^{i\omega(\tau)\tau} = \frac{Q_m(i\omega(\tau), \tau)}{P_m(i\omega(\tau), \tau)}. \quad (2.3)$$

To avoid singularity, we assume $P_m(i\omega(\tau), \tau) \neq 0, \forall \tau$, This can be easily checked by MAPLE or MATHEMATICA.

Denote $\theta(\tau)$ to be any continuous branch of argument of $\frac{|Q_m(i\omega(\tau), \tau)|}{|P_m(i\omega(\tau), \tau)|}$ such that $\theta(\tau_0) \in [0, 2\pi)$ for some τ_0 . Such $\theta(\tau)$ may not be unique but we take only the one with smallest values and the others are indeed of the form $\theta(\tau) + 2k\pi, k = 1, 2, \dots$. Combining this together with (2.3), we have

$$\omega(\tau) = \theta(\tau) + 2n\pi, n = 0, 1, 2, \dots \quad (2.4)$$

Define a sequence of maps $\tau_n : [0, \tau_m] \rightarrow \mathbb{R}_+$ and $S_n : [0, \tau_m] \rightarrow \mathbb{R}$ given by

$$\tau_n(\tau) := \frac{\theta(\tau) + 2n\pi}{\omega(\tau)}, n = 0, 1, 2, \dots \quad (2.5)$$

and

$$S_n := \tau - \tau_n(\tau), n = 0, 1, 2, \dots \quad (2.6)$$

One should notice that all these maps are continuous and differentiable by the assumptions.

The following theorem is the main result of this section. A proof can be found in [Beretta & Kuang 2002].

Theorem 2.1 (Beretta-Kuang 2000): *Assume that $\omega(\tau)$ is a positive real root of $F(\omega, \tau)$ defined for $\tau \in I$, and τ^* is a zero of $S_n(\tau)$ for some $n \in N_0$. Then a pair of simple conjugate pure imaginary roots $\lambda_+(\tau^*) = i\omega(\tau^*)$ and $\lambda_-(\tau^*) = -i\omega(\tau^*)$ exists at $\tau = \tau^*$ which crosses the imaginary axis from left to right if $\delta(\tau^*) > 0$ and crosses the imaginary axis from right to left if*

$\delta(\tau^*) < 0$, where

$$\delta(\tau^*) = \operatorname{sgn} \left\{ \frac{d \operatorname{Re} \lambda}{d\tau} \Big|_{\lambda=i\omega(\tau^*)} \right\} = \operatorname{sgn} \{F_\omega(\omega\tau^*, \tau^*)\} \operatorname{sgn} \left\{ \frac{d \operatorname{Re} S_n(\tau)}{d\tau} \Big|_{\tau=\tau^*} \right\}. \quad (2.7)$$

2.B Introduction to DDE-BIFTOOL: a MATLAB package for bifurcation analysis of DDEs

A large number of numerical packages exist for bifurcation analysis of ordinary differential equations, such as AUTO, LocBif, XPPAUTO, while for delay differential equations only a few exist. Among these DDE-BIFTOOL version 2.00 is the most powerful one, which is introduced by K. Engelborghs, T. Luzyanina and G. Samaey in 2001. The main purpose of the package is to provide a tool for numerical bifurcation analysis of steady state solutions and periodic solutions of equations with constant delays and state-dependent delays. It allows to compute branches of steady state, steady state fold and Hopf bifurcations using continuation method. Given an equilibrium, it can approximate the rightmost characteristic roots on the complex plane which determine stability of the equilibrium. In addition, periodic solutions and approximations of Floquet multipliers can be computed using Lagrange polynomials and adaptive mesh selection. Furthermore, branches of periodic solutions accompany with Hopf bifurcations can be initially guessed and extended globally. It also manages to detect and compute period doubling solutions, homoclinic and heteroclinic in some cases [K. Engelborghs & Roose 2002]

2.C Global Hopf bifurcation with delay independent parameters: HTLV-I infection with CTL response

2.C.1 Model Of HTLV-I infection with CTL response

Mathematical models for Human T-cell leukemia virus type I (HTLV-I) have been widely studied [Osame *et al.* 1990], [Kubota *et al.* 2000], [Bangham 2000]. These viruses prefer to infect CD4+ T cells, causing a strong HTLV-I specific immune response from CD8+ cytotoxic T cells (CTLs), while on the other hand, CTL protectively regulates the proviral load and ultimately leads to HAM/TSP [Bangham 2000]. Recently, many studies focused on dynamics of such mathematical models, including local and global analysis of steady states and limit cycles [Wodarz & Bangham 2000], [Wang *et al.* 2007], [Li & Shu 2010b], [Li & Shu 2010a]. Here we denote x to be the number of uninfected CD4+ target T cells, y to be the number of infected CD4+ target T cells, and z to be the number of HTLV-1 specific CTLs, then the HTLV-1 infection model is provided by

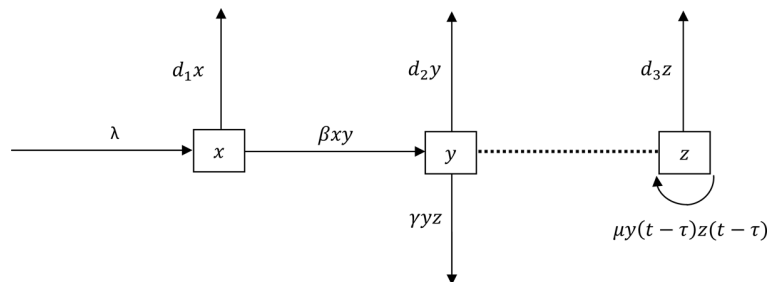


Figure 2.1: Transfer diagram of CTL response to HTLV-I infection.

$$\begin{aligned}
x'(t) &= \lambda - d_1x(t) - \beta x(t)y(t), \\
y'(t) &= \beta x(t)y(t) - d_2y(t) - \gamma y(t)z(t), \\
z'(t) &= \mu y(t - \tau)z(t - \tau) - d_3z(t).
\end{aligned} \tag{2.8}$$

In this system, the parameter λ is the recruitment rate of healthy CD4⁺ T cells from bone marrow. The parameter β is the transmission rate via cell-to-cell contact. The infected CD4⁺ cells are eliminated by CTLs at the rate γ . The strength of CTL response to HTLV-1 infection at time t is assumed to be $\mu y(t - \tau)z(t - \tau)$, which depends on the number of CTLs and infected target cells τ time ago. The delay τ is the period of a few important events such as antigenic activation, selection, and proliferation of CTLs.

2.C.2 Stability analysis

Denote $\mathcal{C}^+ = C([- \tau, 0], \mathbb{R}_+)$. In (2.8), only y and z have delays, thus the solution space is $\mathbb{R} \times \mathcal{C} \times \mathcal{C}$. In order to be biologically meaningful, we should choose the initial condition of the following kind.

$$\phi \in \mathbb{R}_+ \times \mathcal{C}^+ \times \mathcal{C}^+, \quad \phi(0) > 0. \tag{2.9}$$

The following result establishes the feasible region of the model and shows that the model is well-posed. Proof can be found in [Li & Shu 2010b].

Proposition 2.1: *If the initial condition is chosen to be one satisfying (2.9), all solutions of system (2.8) are positive and ultimately bounded in $\mathbb{R} \times \mathcal{C} \times$*

C. Furthermore, all solutions eventually enter and remain in the following bounded and positively invariant region:

$$\Gamma = \left\{ (x, y, z) \in \mathbb{R}_+ \times \mathcal{C}^+ \times \mathcal{C}^+ : |x| \leq \frac{\lambda}{d_1}, \|x + y\| \leq \frac{\lambda}{\tilde{d}}, \|x + y + \frac{\gamma}{\mu} z\| \leq \frac{\lambda}{d} \right\},$$

where $d = \min\{d_1, d_2, d_3\}$ and $\tilde{d} = \min\{d_1, d_2\}$.

System(2.8) has three possible equilibria: the infection free equilibrium $P_0 = (\lambda/d_1, 0, 0)$, the carrier equilibrium $P_1 = (\frac{d_2}{\beta}, \frac{d_1(R_0-1)}{\beta}, 0)$, and the HAM/TSP equilibrium $P_2 = (x^*, y^*, z^*)$, where

$$x^* = \frac{d_2 R_1}{\beta}, \quad y^* = \frac{d_3}{\mu}, \quad z^* = \frac{d_1 d_2 \mu + \beta d_2 d_3}{(d_1 \mu + \beta d_3) \gamma} (R_1 - 1); \quad (2.10)$$

$$\frac{\lambda \beta}{d_1 d_2} =: R_0 > R_1 := \frac{\lambda \beta \mu}{d_1 d_2 \mu + \beta d_2 d_3}. \quad (2.11)$$

In fact, these R_0, R_1 completely determine the existence and global stability of P_0 and P_1 [Li & Shu 2010a], [Li & Shu 2010b], which is shown in the following theorem.

Theorem 2.2: *(i) If $R_0 \leq 1$, then P_0 is the only equilibrium and it is globally asymptotically stable. Thus viruses are cleaned away.*

(ii) If $R_1 \leq 1 < R_0$, then P_0 is unstable the carrier equilibrium P_1 is the only chronic-infection equilibrium and is globally asymptotically stable. The patient remains as an asymptotic carrier.

(iii) If $R_1 > 1$, then P_0, P_1 are unstable, and the HAM/TSP equilibrium P_2 exists. Both the HTLV-I infection and the CTL response are persistent. The patient has high risk to develop HAM/TSP.

In the following context, we focus on the HAM/TSP equilibrium P_2 , which exists only when $R_1 > 1$. Thus we always assume $R_1 > 1$. To explore its stability, we first linearize system (2.8) about P_2 , and we obtain the following linear system.

$$\begin{aligned}x'(t) &= -(\beta y^* + d_1)x(t) - \beta x^* y(t), \\y'(t) &= \beta y^* x(t) - \gamma y^* z(t), \\z'(t) &= \mu z^* y(t - \tau) + d_3 z(t - \tau) - d_3 z(t).\end{aligned}\tag{2.12}$$

The characteristic equation associated with (2.12) is

$$D(\xi) := P(\xi) + Q(\xi) e^{-\xi\tau} := \xi^3 + a_2 \xi^2 + a_1 \xi + a_0 + (b_2 \xi^2 + b_1 \xi + b_0) e^{-\xi\tau} = 0,\tag{2.13}$$

where

$$\begin{aligned}a_2 &= d_3 + \beta y^* + d_1, & a_1 &= d_3(\beta y^* + d_1) + \beta^2 x^* y^*, & a_0 &= \beta^2 x^* y^* d_3, \\b_2 &= -d_3, & b_1 &= \gamma d_3 z^* - d_3(\beta y^* + d_1), & b_0 &= \gamma d_3 z^*(\beta y^* + d_1) - \beta^2 x^* y^* d_3.\end{aligned}$$

When $\tau = 0$, (2.13) becomes

$$\xi^3 + (a_2 + b_2)\xi^2 + (a_1 + b_1)\xi + (a_0 + b_0) = 0.$$

Noticing that

$$\begin{aligned}
a_0 + b_0 &= \gamma d_3 z^* (\beta y^* + d_1) > 0, \\
a_1 + b_1 &= \gamma d_3 z^* + \beta^2 x^* y^* > 0, \\
a_2 + b_2 &= \beta y^* + d_1 > 0, \\
(a_2 + b_2)(a_1 + b_1) - (a_0 + b_0) &= \beta^2 x^* y^* (\beta y^* + d_1) > 0.
\end{aligned}$$

and according to Routh-Hurwitz criterion, we know that all characteristic roots have negative real parts when $\tau = 0$. Hence the HAM/TSP equilibrium P_2 is locally asymptotically stable when $\tau = 0$.

For $\tau > 0$, as the method described in the previous section, we assume that the characteristic equation (2.13) has a pair of conjugate pure imaginary roots $\xi = i\omega$ ($\omega > 0$), then ω is a positive root of the following polynomial that is independent of τ :

$$\begin{aligned}
F(\omega) &:= |P(i\omega)|^2 - |Q(i\omega)|^2 \\
&= \omega^6 + (a_2^2 - b_2^2 - 2a_1)\omega^4 + (a_1^2 - 2a_0a_1 - b_1^2 + 2b_0b_2)\omega^2 + (a_0^2 - b_0^2)
\end{aligned} \tag{2.14}$$

Let $G(u) = F(\sqrt{u})$, which is a cubic polynomial. We see that $i\omega$ ($\omega > 0$) is a root of $F(\omega)$ if and only if $u = \omega^2$ is a positive root of $G(u)$.

We then obtain the following equation about τ :

$$e^{i\omega\tau} = -\frac{Q(i\omega)}{P(i\omega)} \tag{2.15}$$

whose solutions are

$$\tau_n = \frac{1}{\omega} \arg \left\{ -\frac{Q(i\omega)}{P(i\omega)} \right\} + \frac{2n\pi}{\omega}, \quad n \in \mathbb{N}. \quad (2.16)$$

Here \arg is a continuous fork of arguments containing a positive interval.

According to Beretta and Kuang's method[Beretta & Kuang 2002], since the polynomials P , Q , F , G do not depend on τ , we have the following result:

$$\operatorname{sgn} \left\{ \frac{d\operatorname{Re}\xi}{d\tau} \Big|_{\xi=i\omega, \tau=\tau_n} \right\} = \operatorname{sgn}\{G'(\omega^2)\}. \quad (2.17)$$

Since $G(u)$ is a cubic polynomial. there may be zero, one, two or three positive roots, said $\omega_1 > \omega_2 > \omega_3$, which then result in none, one, two, or three different $S_n(\tau)$ and τ_n sequences, said τ_n^1 , τ_n^2 and τ_n^3 respectively. In any case, a pair of conjugate complex roots pass the imaginary axis to the right as τ increases to τ_1^n or τ_3^n , for any $n = 0, 1, 2, \dots$, while a pair of conjugate complex roots pass the imaginary axis to the left where τ reaches τ_n^2 , for any $n = 0, 1, 2, \dots$. Notice that the possible three roots of $G(u)$, $\omega_1, \omega_2, \omega_3$ have the order $\omega_1 > \omega_2 > \omega_3$, thus the order of the differences of the three τ -sequences is $2\pi/\omega_1 < 2\pi/\omega_2 < 2\pi/\omega_3$, i.e., the τ_n^1 is more dense than τ_n^2 and τ_n^3 . So as τ increases from 0, the first critical value reached is τ_0^1 , and then follows τ_0^2 or τ_1^1 . Furthermore, there exists a τ_c , such that for all $\tau > \tau_c$, there will be characteristic roots with positive real parts, which means that P_2 is ultimately unstable when τ is large enough. This is the common law of all delayed models with delay independent parameters, and is the main difference to delayed models with delay dependent parameters discussed in the next section. The following theorem reveals the stability of P_2 , which is

proved in [Li & Shu 2010a].

Theorem 2.3: *(Stability of P_2)*

- (1) *If $G(u)$ has no positive real root, then there is no stability switch, and the stability of p_2 stays the same as when $\tau = 0$, i.e., delay has no effect on stability of P_2 .*
- (2) *If $G(u)$ has at least one positive root, and P_2 is unstable when $\tau = 0$, then for any τ , P_2 is unstable, i.e., no stability switch or Hopf bifurcation.*
- (3) *If $G(u)$ has at least one positive root and P_2 is stable when $\tau = 0$, then P_2 will experience a sequence of stability switches (finitely many times yet at least one), and after some τ_c , it stays unstable as τ increases, i.e., for τ large enough, P_2 is unstable.*

These results show that large time delay can add instability and oscillations to the dynamical system. However, small τ value is harmless, due to continuity property and the implicit function theorem.

According to the Hopf bifurcation theorem, these τ values are Hopf bifurcation points where periodic solutions accompany as characteristic roots cross the imaginary axis. It is interesting to track the behaviors of the Hopf branches as τ increases. Overlaps of branches can be expected, where we can get multiple periodic solutions at with a some τ , even multiple stable periodic solutions, which may be more biologically interesting

Since the number of positive roots of $G(u)$ can be zero, one, two or three, we need to discuss the global behaviors of Hopf branches in each case separately. Obviously, we do not need to discuss the case when $G(u)$ has no positive real

root. For the case when $G(u)$ has only one positive solution, Hopf branches arising from τ_n^1 go unbounded when τ increase from 0 to infinity, which has been shown and proved [Wu 1998], [Wei & Li 2005]. For cases when there are more than one positive roots, theory has not yet been established. What we do here is to do numerical simulations on chosen parameters using the DDE-BIFTOOL MATLAB package.

2.C.3 Stability switch and global Hopf bifurcation case

I: $G(u)$ has two positive roots

This case has been fully explored by Li and Shu in their recent paper [Li & Shu 2010a]. Here we choose a different group of parameters shown below to obtain a larger overlap τ -interval of stable branches in Figure 2.3.

$$\begin{aligned} \lambda = 160, \beta = 0.002, \gamma = 0.2, \mu = 0.2, \\ d_1 = 0.16, d_2 = 1.845, d_3 = 0.5. \end{aligned} \tag{2.18}$$

Then $G(u)$ has 2 positive solutions ω_1^2, ω_2^2 (Figure 2.2), with

$$\omega_1 = 0.0858 > \omega_2 = 0.1950.$$

From (2.16), we obtain two τ -sequences

$$\begin{aligned} \tau^1 &= \{0.889209, 33.1177, 65.3461, 97.5745, 129.803, \dots\}, \\ \tau^2 &= \{13.2443, 86.5094, 159.775, 233.04, 306.305, \dots\}, \end{aligned}$$

with respect to ω_1 and ω_2 . When $\tau = 0$, the system becomes an ODE, and the

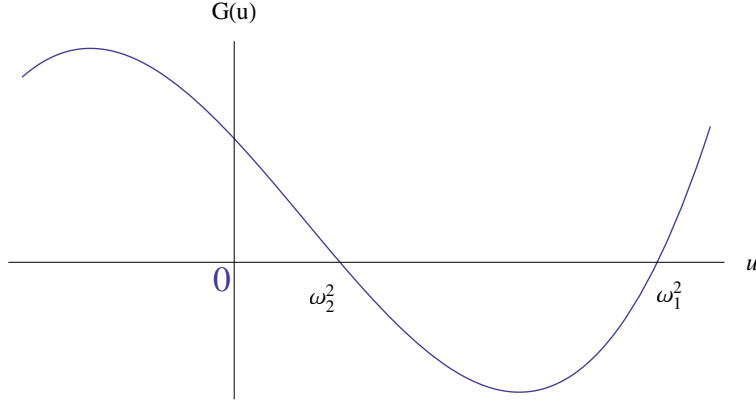


Figure 2.2: Graph of $G(u)$ with two positive roots.

three characteristic roots are -0.1444 , $-0.0103 \pm 0.2320i$, which imply that P_2 is stable when $\tau = 0$.

From Theorem 2.3, as τ increases, the HAM/TSP equilibrium P_2 is stable when $\tau < \tau_0^1$, and it is unstable in $[\tau_0^1, \tau_0^2]$, stable again in $[\tau_0^2, \tau_1^1]$, and after τ_1^1 , it stays unstable. From the bifurcation theorem, we know that Hopf branches bifurcating from τ_0^1 and τ_0^2 are stable around these bifurcation values, and these two branches are shown to connect with each other, i.e., τ_0^1, τ_0^2 are connected by a single stable Hopf branch. Similarly, $\tau_n^1 (n \geq 1)$ is also connected with the corresponding τ_n^2 by a single Hopf branch, whose stability may vary for different τ values. Indeed, what makes this problem interesting is that the τ sequences are derived from the linearization around P_2 which is a local property, but Hopf branches are global! Whatsoever, a rigorous mathematical proof has not yet been done, and we do not know how common such a phenomenon is. Another observation from Figure 2.3 is that when $\tau_2^1 < \tau < \tau_1^2$, there is an overlap of two branches, i.e., two periodic solutions. Furthermore, these two branches have their stable τ intervals, and these intervals have a small overlap, which means that in this overlap interval, the two periodic solu-

tions are both stable. DDE23 is used here to confirm their existence. Results are shown in Figure 2.4 and Figure 2.5

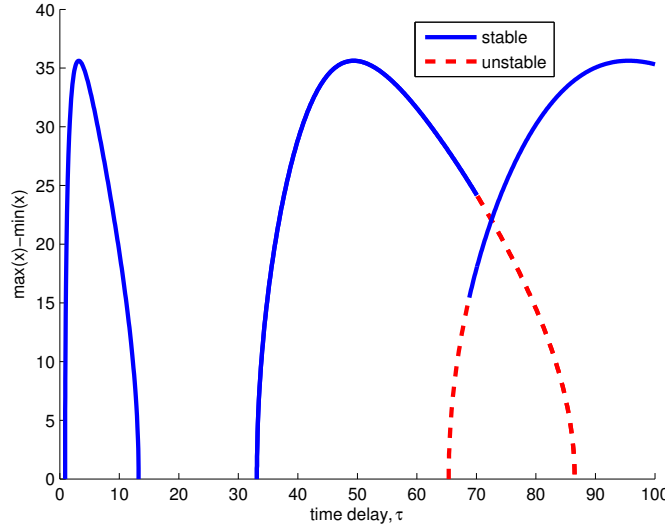


Figure 2.3: Bifurcation diagram showing stability switches at P_2 and global Hopf branches bifurcating from those switches τ values. Parameters are given as follows: $\lambda = 160$, $\beta = 0.002$, $\gamma = 0.2$, $\mu = 0.2$, $d_1 = 0.16$, $d_2 = 1.845$, $d_3 = 0.5$.

Another observation we get from Figure 2.3 is that periodic solutions on the last two Hopf branches change their stability at some τ 's. This phenomenon is called secondary bifurcation, on which mathematical theories are not well developed. To find the types of these secondary bifurcations, we track the development of Floquet multipliers of these periodic orbits and find that on both branches, there are a pair of non-real complex Floquet multipliers crossing the unit circle (Figure 2.6), therefore secondary bifurcations on both branches are torus bifurcations, i.e., on each branch, there is an invariant torus on the neighborhood of the periodic solution, when τ stays close to the secondary bifurcation value.

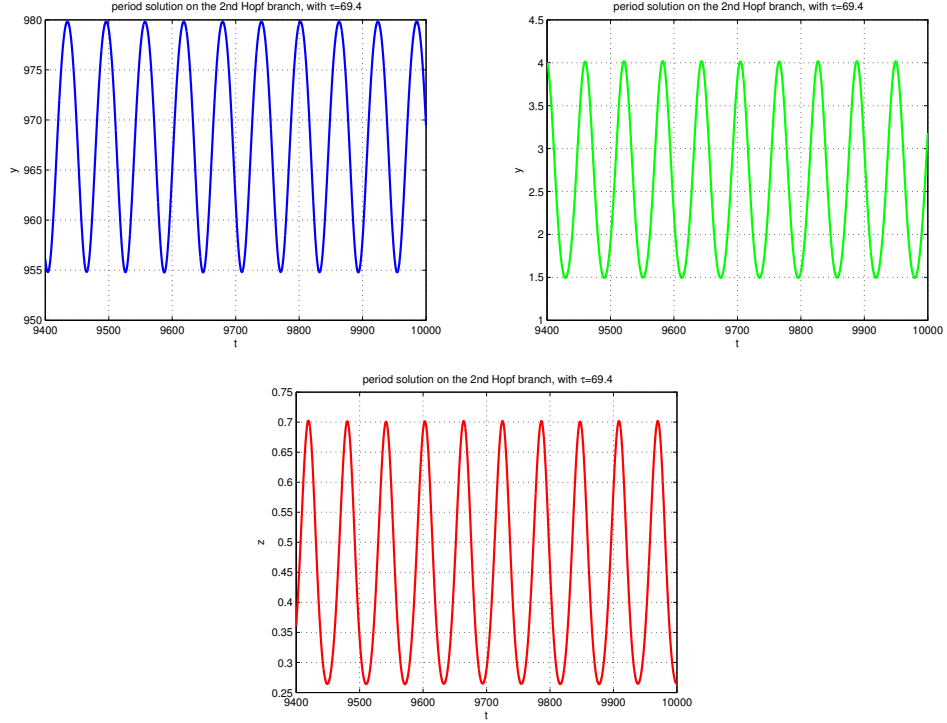


Figure 2.4: Periodic solution on the 2nd Hopf branches in the overlap stable interval in Figure 2.3, with $\tau = 69.4$. Period of this solution is about 61.1.

2.C.4 Stability switch and global Hopf bifurcation case

II: $G(u)$ has three positive roots

For this case, we choose the following set of parameter values:

$$\lambda = 60, \beta = 0.17, \gamma = 0.2, \mu = 0.15, d_1 = 0.85, d_2 = 1.85, d_3 = 0.35. \quad (2.19)$$

Then $G(u)$ has three positive solutions (Figure 4)

$$\omega_1^2 = 3.4011 > \omega_2^2 = 1.2046 > \omega_3^2 = 0.3311.$$

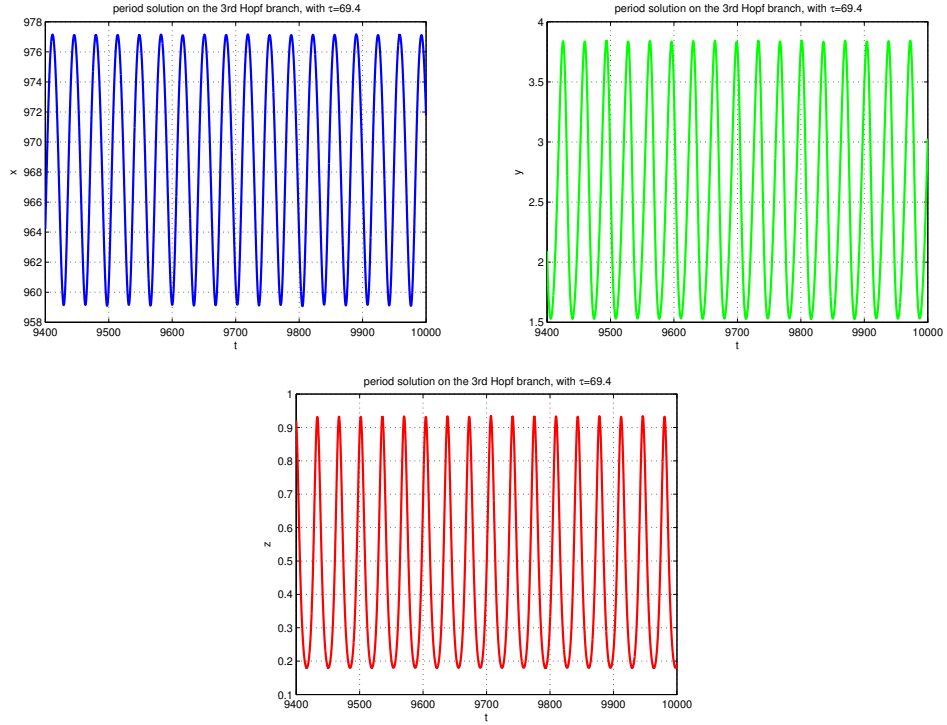


Figure 2.5: Periodic solution on the 3rd Hopf branches in the overlap stable interval in Figure 2.3, with $\tau = 69.4$. Period of this solution is about 34.2.

From (2.16), we obtain three sequences of solutions

$$\tau^1 = \{0.532192, 3.93919, 7.34619, 10.7532, 14.1602, \dots\},$$

$$\tau^2 = \{1.86833, 7.59318, 13.318, 19.0429, 24.7677, \dots\},$$

$$\tau^3 = \{4.18349, 15.103, 26.0226, 36.9421, 47.8617, \dots\},$$

with respect to ω_1 , ω_2 , and ω_3 , respectively.

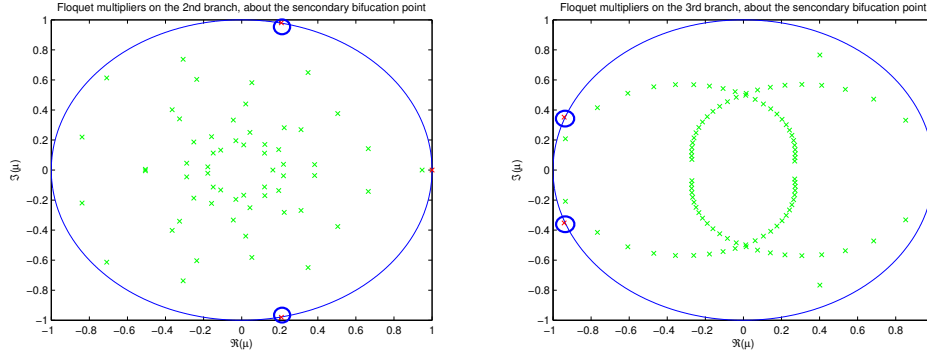


Figure 2.6: Floquet multipliers for periodic solutions around secondary bifurcation points on the second branch (left) and the third branch (right) as shown in Figure 2.3 .

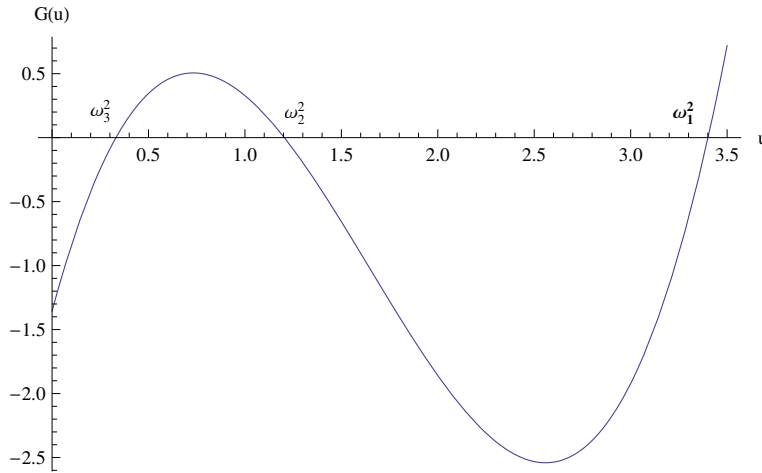


Figure 2.7: Graph of $G(u)$ with three positive roots.

Global Hopf branches

With DDE-BIFTOOL package, we compute Hopf branches at bifurcation values of τ in each of the sequences and globally extend the local branches. As shown in Figure 5, we see again that a family of bounded global Hopf branches connecting a pair of bifurcation points at τ_n^1 and τ_n^2 . A second family of Hopf branches originate from bifurcation points at τ_n^3 in the third sequence, and

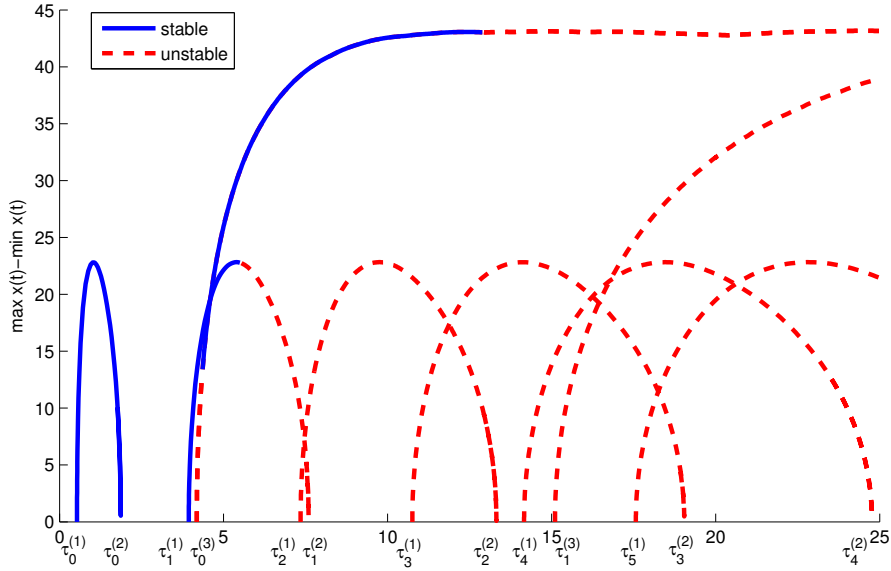


Figure 2.8: Bifurcation diagram showing stability switch at P_2 and the global Hopf branches, with parameters given in (2.19). Solid lines indicate stable branches, and dashed lines indicate unstable branches.

these branches appear to be unbounded in all of our computations.

The behavior of the global Hopf branches originates from the third sequence τ_n^3 may be reminiscent of that of the global Hopf branches when $G(u)$ has a single positive root and there is a single sequence of bifurcation values for τ . Such phenomenon was investigated in a delayed Nicholson blowflies equation in [Wei & Li 2005], and the authors rigorously established that all global Hopf branches are unbounded.

Coexistence of multiple stable periodic solutions

In Figure 5, a solid line indicates stable part of a Hopf branch and a dashed line unstable. We see that the second bifurcation value τ_1^1 in the first sequence precedes and first value τ_0^3 of the third sequence, so the order of the two

sequences crosses over, producing an overlap of two Hopf branches. We also observe that two solid portions from the branches overlap. This indicates that there exists an open interval of τ values between τ_1^1 and τ_0^3 for which there are two stable periodic solutions.

We use DDE23 package of Matlab to numerically solve system (2.8) for the set of parameter values in (2.19) and for τ values around 5, which is in the overlapping region. In Figure 6, we show two periodic solutions, for the same set of parameter values and same value of delay τ , corresponding to different initial conditions. Nearby solutions have been observed to converge to these solutions so that they are stable. We have also numerically computed the Floquet multipliers for each of the periodic solutions and, except for the multiplier 1, all of the multipliers stay inside the unit circle, indicating that both periodic solutions are stable.

It is apparent from Figure 6 that the two periodic solutions are different in their periods and amplitudes.

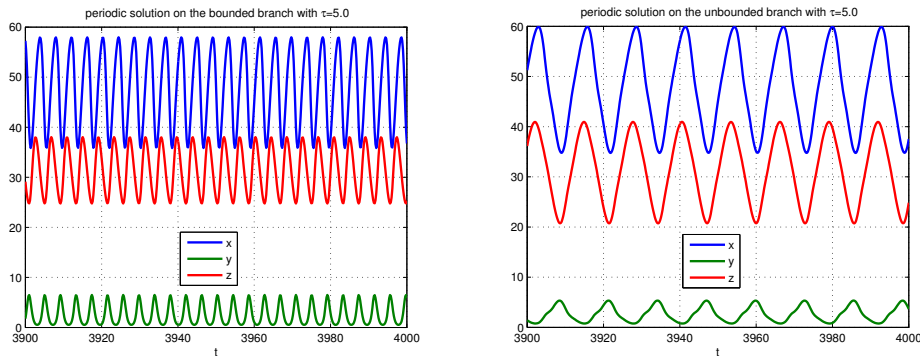


Figure 2.9: Two stable periodic solutions for the same set of parameters and same delay $\tau = 5$.

Secondary bifurcations

In Figure 5, along the unbounded Hopf branch at the bifurcation value τ_0^3 , when τ is sufficiently large, the solid line changes to dashed line at $\tau = \tau_s$, indicating a change in stability of the periodic solutions, and that a secondary bifurcation may have occurred from the periodic solution at τ_s . Analysis on the periodic orbit around the secondary bifurcation value τ_s reveals that a Floquet multiplier crosses the unit circle from interior to exterior at -1 , indicating that a period-doubling bifurcation occurs.

DDE-BIFTOOL package is used to further investigate the secondary bifurcations along this branch near τ_s , and we discover that a period-doubling cascade occurs. In Figure 7, we show simulation results using DDE23 of for periodic solutions for $\tau = 12, 15, 23$, and 100 , whose periods show the doubling effect.

It is known that a period-doubling cascade may eventually lead to chaos. We explored this possibility using power spectrum of Fourier transforms of solutions along this branch. However, we did not detect a wide band of spectrum typical of chaotic solutions. From a projected orbit and a power spectrum shown in Figure 8, the period doubling may lead to a quasi-periodic solution. This needs to be further investigated in future studies.

2.C.5 Summary and discussion on the HTLV-I infection model

In this study, we examine Hopf bifurcations in a mathematical model of immune response to retroviral infections with time delay when the delay τ is

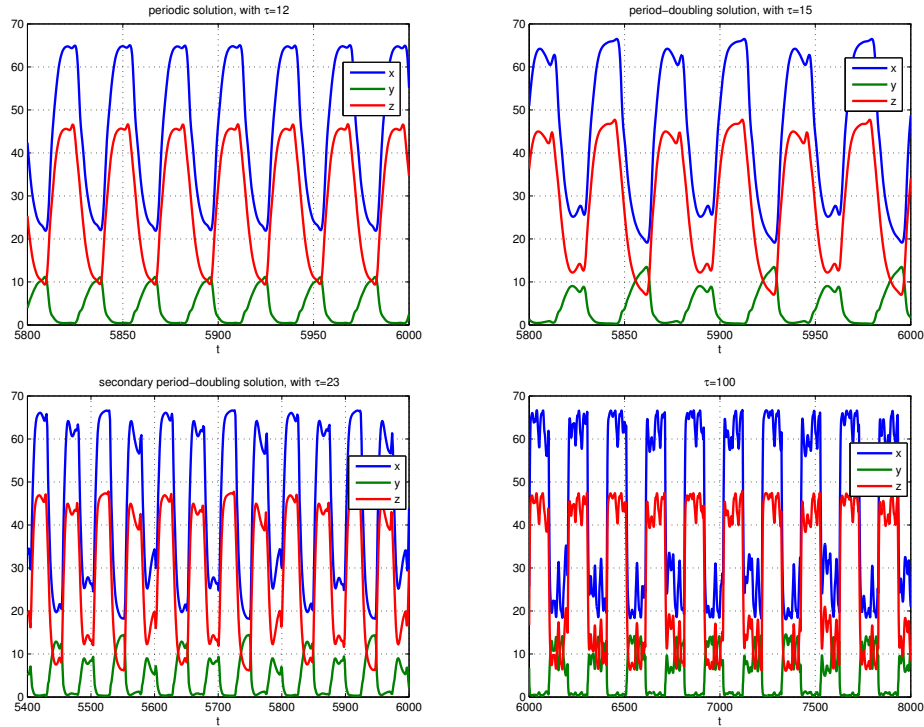


Figure 2.10: Four periodic solutions for $\tau = 12, \tau = 15, \tau = 23, \tau = 100$ showing the period-doubling effect.

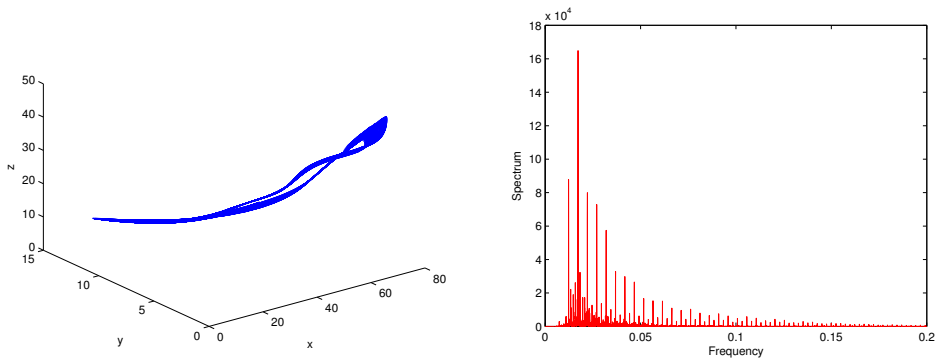


Figure 2.11: Projection of the periodic solution in Figure 7 with $\tau = 100$ to the xyz -space and its power spectrum from FFT.

varied. Our results reveal that when two sequences of Hopf bifurcation values exist, the phenomenon of stability switch occurs. Furthermore, a family of bounded global Hopf branches exist and an overlap of these branches may

lead to coexistence of multiple stable periodic solutions.

This study also characterizes the global Hopf branches when there are three sequences of Hopf bifurcation values. In this case, we show that, for the first time, in addition to the family of bounded global Hopf branches, a family of unbounded global Hopf branch exists. We also show that period-doubling secondary bifurcations may occur along this unbounded branch.

Our analysis and results reveal that stability along the global Hopf branches may change and lead to different types of secondary bifurcations and creation of more complex and interesting solutions. Further studies are needed to explore possible secondary bifurcations along the global Hopf branches.

We would like to point out that though our study was carried out for a particular mathematical model, behaviors of this nature should be universal and may exist in other systems with time delays. In fact, similar analysis and simulations are also carried out with the following HIV model in which the same phenomena are observed.

$$\begin{aligned}
 \frac{dT}{dt} &= s - \alpha T + rT \left(1 - \frac{T + T^*}{M} \right) - kT(t - \tau)V(t - \tau) \\
 \frac{dT^*}{dt} &= kT(t - \tau)V(t - \tau) - \beta T^* \\
 \frac{dV}{dt} &= N\beta T^* - \gamma V
 \end{aligned} \tag{2.20}$$

where T , T^* and V are amount of healthy T-cells, infected T-cells and HIV virus respectively. The delay denotes the time lag that a healthy T-cell becomes infected after contacted with an infected T-cell.

2.D Global Hopf bifurcation with delay dependent parameters : delayed Lotka-Volterra model

2.D.1 Delayed Lotka-Volterra model

The delayed Lotka-Volterra system is described as the following.

$$\begin{aligned}x'(t) &= rx(t) \left(1 - \frac{x(t)}{K}\right) - \beta f(x(t))y(t), \\y'(t) &= \gamma\beta e^{-d_j\tau} f(x(t-\tau))y(t-\tau) - dy(t),\end{aligned}\tag{2.21}$$

where the response function $f(x) = xg(x)$ is increasing for all $x > 0$. Examples of $f(x)$ are Holling Type functions:

$$f(x) = x, f(x) = \frac{x}{D+x}, f(x) = \frac{x^m}{D^m+x^m} \quad (m > 1).$$

Nondimensionalization can be done to make the system become

$$\begin{aligned}x'(t) &= x(t)(1-x(t)) - f(x(t))y(t), \\y'(t) &= \gamma e^{-d_j\tau} f(x(t-\tau))y(t-\tau) - dy(t).\end{aligned}\tag{2.22}$$

There are three possible equilibria, $P_0 = (0, 0)$, $P_1 = (1, 0)$ and $P_2 = (x^*, y^*)$, where

$$x^* = f^{-1}\left(\frac{d}{\gamma}e^{d_j\tau}\right) > 0, \quad y^* = \frac{x^*(1-x^*)}{f(x^*)} = \frac{\gamma x^*(1-x^*)}{de^{d_j\tau}} > 0.\tag{2.23}$$

Existence of P_0 and P_1 is unconditional, while P_2 exists if and only if

$$\frac{d}{\gamma} e^{d_j \tau} < f(1) \quad \Leftrightarrow \quad R(\tau) := \frac{\gamma f(1)}{d} e^{-d_j \tau}, \quad (2.24)$$

or equivalently,

$$\tau < \tau_m := \frac{1}{d_j} \log \frac{\gamma f(1)}{d} \quad \text{and} \quad R_0 := R(0) = \frac{\gamma f(1)}{d} > 1.$$

$R(\tau)$ is called the basic reproduction number. We will see later R_0 and $R(\tau)$ significantly affect the dynamics of the system. This is biologically clear as one can see that the basic reproduction number $R(\tau)$ is simply the ratio of the possible maximum recruitment rate to adulthood ($\gamma e^{-d_j \tau} f(1)$) against the death rate of adults (d).

For P_0 , since on the manifold where $y \equiv 0$, this system can be reduced to be

$$x'(t) = x(1 - x),$$

and $x = 1$ is unstable. Thus P_0 is unstable.

Theorem 2.4 (Positivity and boundedness): *Given any positive initial condition, i.e., $\phi \in \mathcal{C}^+ \times \mathcal{C}^+$, $\phi(0) > 0$, all solutions of system (2.22) are positive and ultimately bounded in $\mathcal{C}^+ \times \mathcal{C}^+$. Specifically, all trajectories eventually enter and remain in the following positive and bounded invariant region.*

$$\Gamma = \left\{ (x, y) \in \mathcal{C}^+ \times \mathcal{C}^+ : \|x\| \leq 1, \|y\| < \frac{\gamma e^{-d_j \tau}}{\min\{1, d\}} \right\}.$$

Proof. Positivity is obvious by Theorem (1.6). We only show boundedness

here. Since

$$x'(t) \leq x(1 - x),$$

By the comparison theorem and boundedness of the logistic model($y \equiv 0$), we know that $x(t)$ is ultimately bounded by 1, i.e.,

$$\limsup_{t \rightarrow +\infty} x(t) \leq 1.$$

Therefore, all solutions will eventually enter and remain in

$$\Gamma' = \{(x, y) \in \mathcal{C}^+ \times \mathcal{C}^+ : \|x\| \leq 1\}.$$

Add the two equations of (2.22). For any $(x, y) \in \Gamma'$, we have

$$\begin{aligned} (\gamma e^{-d_j \tau} x(t) + y(t + \tau))' &= \gamma e^{-d_j \tau} x(t)(1 - x(t)) - dy(t + \tau) \\ &\leq \gamma e^{-d_j \tau} (1 - x(t)) - dy(t + \tau) \\ &\leq \gamma e^{-d_j \tau} - \min\{1, d\} (\gamma e^{-d_j \tau} x(t) + y(t + \tau)). \end{aligned}$$

Thus we have

$$\limsup_{t \rightarrow +\infty} (\gamma e^{-d_j \tau} x(t) + y(t + \tau)) \leq \frac{\gamma e^{-d_j \tau}}{\min\{1, d\}}.$$

Since $x(t) > 0$ for all $t > 0$, we have

$$\limsup_{t \rightarrow +\infty} y(t) \leq \frac{\gamma e^{-d_j \tau}}{\min\{1, d\}}.$$

i.e., all solutions in Γ' will finally enter and remain in Γ . □

2.D.2 Stability of the boundary equilibrium P_1

To linearize system (2.22) around $P_1 = (1, 0)$, let $u = x - 1$, $v = y$, then the corresponding linear system is

$$\begin{aligned} u'(t) &= -u(t) - f(1)v(t), \\ v'(t) &= -dv(t) - \gamma e^{-d_j \tau} f(1)v(t - \tau). \end{aligned} \tag{2.25}$$

Assume system (2.25) has solution of the form

$$u = u_0 e^{\lambda t}, \quad v = v_0 e^{\lambda t}.$$

Plug these into (2.25), and we get the following characteristic equation.

$$\begin{aligned} D_1(\lambda, \tau) &= \lambda^2 + (d + 1)\lambda + d - \gamma f(1)e^{-d_j \tau}(\lambda + 1)e^{-\lambda \tau} \\ &= (\lambda + 1)(\lambda + d - \gamma f(1)e^{-d_j \tau}e^{-\lambda \tau}). \end{aligned} \tag{2.26}$$

Theorem 2.5: (*Stability of P_1*)

(1) If $R(\tau) \leq 1$, i.e.,

$$R_0 \leq 1 \quad \text{or} \quad R_0 > 1 \quad \text{and} \quad \tau \geq \tau_m,$$

the interior equilibrium does not exist and $P_1(1, 0)$ is globally asymptotically stable;

(2) If $R(\tau) > 1$, i.e.,

$$R_0 > 1 \quad \text{and} \quad \tau \leq \tau_m,$$

$P_1(1, 0)$ is unstable.

Proof. 1) Let $c := \gamma e^{-d_j \tau} f(1) \geq d$. Since Γ is globally attracting, we need

only to consider solution $(x_t, y_t) \in \Gamma$, then

$$\begin{aligned}\frac{dy}{dt} &= \gamma e^{-d_j \tau} f(x(t)) y(t - \tau) - dy(t) \\ &\leq \gamma e^{-d_j \tau} f(1) y(t - \tau) - dy(t) \\ &= cy(t - \tau) - dy(t).\end{aligned}$$

Construct a Lyapunov function

$$V(y(t)) = \frac{1}{2} y^2(t) + \frac{c}{2} \int_{t-\tau}^t y^2(s) ds.$$

We have $V(0) = 0$, $V(y(t)) \geq 0$, and

$$\begin{aligned}\frac{dV(y(t))}{dt} &= y(t) y'(t) + \frac{c}{2} (y^2(t) - y^2(t - \tau)) \\ &\leq cy(t) y(t - \tau) - dy^2(t) + \frac{c}{2} (y^2(t) - y^2(t - \tau)) \\ &\leq \frac{c}{2} (y^2(t) + y^2(t - \tau)) - dy^2(t) + \frac{c}{2} (y^2(t) - y^2(t - \tau)) \\ &= (c - d) y^2(t) \leq 0.\end{aligned}$$

0 is attained only if $x(t) = 1$ from the first shrinking. Assume $x(t_0) = 1$. If $y(t_0) \neq 0$, by the comparison theorem, $x(t) < 1$ for $t > t_0$, and $\frac{dV(y(t))}{dt} < 0$ for $t > t_0$. Hence $(1, 0)$ is globally attractive.

2) If $\tau < \tau_m$, then $\gamma e^{-d_j \tau} f(1) < d$. Recall the characteristic equation (2.26) and let $\alpha(\lambda) = \lambda + d - \gamma f(1) e^{-d_j \tau - \lambda \tau}$, then

$$\alpha(0) = d - \gamma f(1) e^{-d_j \tau} < 0, \quad \alpha(+\infty) = d > 0.$$

So there is an $\lambda_0 > 0$, such that $\alpha(\lambda_0) = 0$. So $\lambda_0 > 0$ is a characteristic root. P_0 is unstable. □

Back to the ecosystem, theorem 2.5 implies that if the mature time of juvenile predators is large, predators will go extinct. This is biologically obvious since in this case recruitment rate to adulthood is smaller than its death rate.

2.D.3 Stability of the coexistence equilibrium P_2

To ensure the existence of $P_2 = (x^*, y^*)$, condition (2.24) should be satisfied, i.e., $\gamma f(1) > d$ and

$$\tau < \tau_m := \frac{1}{d_j} \log \frac{\gamma f(1)}{d}.$$

Let $x = x^* + u$, $y = y^* + v$ and $|u|, |v| \ll 1$. The corresponding linear function is

$$\begin{aligned} u'(t) &= (1 - 2x^* - y^* f'(x^*))u(t) - f(x^*)v(t), \\ v'(t) &= \gamma e^{-d_j \tau} y^* f'(x^*)u(t - \tau) + \gamma e^{-d_j \tau} f(x^*)v(t - \tau) - dv(t). \end{aligned} \tag{2.27}$$

We look for solution of the form $(u, v) = (u_0, v_0) e^{\lambda t}$ with $(u_0, v_0) \neq 0$, and get the following characteristic equation.

$$\begin{aligned} D(\lambda, \tau) &= \lambda^2 + a_1 \lambda + a_0 + (b_1 \lambda + b_0) e^{-\lambda \tau} \\ &=: P(\lambda, \tau) + Q(\lambda, \tau) e^{-\lambda \tau}, \end{aligned} \tag{2.28}$$

where

$$a_1 = d + y^* f'(x^*) + 2x^* - 1,$$

$$a_0 = d(a_1 - d),$$

$$b_1 = -d,$$

$$b_0 = -d(2x^* - 1).$$

In the following context, our interest is all possible stability switches as τ increases from zero to τ_m . When $\tau = 0$, the characteristic equation can be simplified to be

$$\lambda^2 + H(0)\lambda + \gamma y^* f(x^*) f'(x^*) = 0, \quad (2.29)$$

where

$$H(\tau) = 2x^* + y^* f'(x^*) - 1.$$

Here we used that fact that when $\tau = 0$, $\gamma f(x^*) = d$.

Notice that $\gamma y^* f(x^*) f'(x^*) > 0$. If $H(0) < 0$, the two solutions of (2.29) both have positive real parts, thus the interior equilibrium is unstable; if $H(0) > 0$, the two solutions both have negative real parts, and the interior equilibrium is stable.

For $\tau > 0$, suppose $D(\lambda, \tau) = 0$ has imaginary solutions of the form $\lambda = i\omega$ ($\omega \neq 0$). Since conjugate roots appear in pairs, we can assume that $\omega > 0$ without losing generality. Substitute it into (2.28) and separate the real and

the imaginary parts, we have

$$b_0 \cos \omega\tau + b_1 \omega \sin \omega\tau = \omega^2 - a_0, \quad (2.30)$$

$$b_1 \omega \cos \omega\tau - b_0 \sin \omega\tau = -a_1 \omega. \quad (2.31)$$

Computing $(2.30)^2 + (2.31)^2$, we get after simplification

$$F(\omega, \tau) := \omega^4 + (a_1 - d)^2 \omega^2 + d^2 y^* f'(x^*) J(\tau) = 0, \quad (2.32)$$

where

$$J(\tau) = y^* f'(x^*) + 4x^* - 2.$$

Let

$$I_- = \{\tau \in (0, \tau_m) : J(\tau) < 0\}, \quad I_+ = \{\tau \in (0, \tau_m) : J(\tau) \geq 0\}.$$

If $I_- = \emptyset$, i.e., $J(\tau) \geq 0, \forall \tau \in (0, \tau_m)$, then $F(\omega, \tau)$ has no positive root for $0 < \tau < \tau_m$, therefore no root will cross the imaginary axis, thus no bifurcation or stability switch occurs. Indeed, one can verify that there is no zero characteristic roots in (2.28) as $a_0 \neq b_0$. Thus even at τ value where $J(\tau) = 0$, there is no bifurcation or stability switch. Since $2H(\tau) = J(\tau) + y^* f'(x^*)$, which implies $H(0) = y^*(0) f'(x^*(0)) > 0$, P_2 is stable when $\tau = 0$, thus stable for $0 \leq \tau < \tau_m$.

If $I_- \neq \emptyset$, then $F(\omega, \tau)$ has one and only one positive solution for $\tau \in I_-$. Stability switches and Hopf bifurcations can only occur in I_- . Following the method described in section 2.A, we can construct a sequence of functions

$S_n(\tau)$, $n = 0, 1, 2, \dots$ and determine stability switches and Hopf bifurcation values by theorem 2.1. It is convenient to notice that $F'_\omega(\omega(\tau^*), \tau^*) > 0$ since $\omega(\tau^*)$ is the largest and single real root and coefficient of the highest order term of $F(\omega, \tau^*)$ is positive. Thus (2.7) can be reduced to

$$\delta(\tau^*) = \operatorname{sgn} \left\{ \left. \frac{d\operatorname{Re} \lambda}{d\tau} \right|_{\lambda=i\omega(\tau^*)} \right\} = \operatorname{sgn} \left\{ \left. \frac{d\operatorname{Re} S_n(\tau)}{d\tau} \right|_{\tau=\tau^*} \right\}. \quad (2.33)$$

In the following two sections, we study the model with Holling Type I and Type II functional responses, mainly on stability switches and Hopf bifurcations about the coexistence equilibrium P_2 as global property of P_1 are already well developed in this session. Results on P_2 which are clear in this section will be given directly without detailed calculations.

2.D.4 Model with Holling Type I functional response: stability and global Hopf bifurcation

Assume $f(x) = x$, then coexistence equilibrium $P_2(x^*, y^*)$ is

$$x^* = \frac{1}{R(\tau)}, \quad y^* = 1 - \frac{1}{R(\tau)},$$

where

$$R_0 = \gamma/d, \quad R(\tau) = R_0 e^{-d_j \tau}.$$

If $R_0 > 1$, $\tau_m = \frac{1}{d_j} \log R_0$. The corresponding characteristic equation is

$$\begin{aligned} D(\lambda) &= P(\lambda, \tau) + Q(\lambda)e^{-\lambda\tau} \\ &= \lambda^2 + \left(d + \frac{1}{R(\tau)} \right) \lambda + \frac{d}{R(\tau)} + \left(-d\lambda + d - \frac{2d}{R(\tau)} \right) e^{-\lambda\tau}. \end{aligned} \quad (2.34)$$

Other quantities are

$$F(\omega, \tau) = \omega^4 + \frac{1}{R(\tau)^2} \omega^2 - \frac{d^2}{R(\tau)^2} (R(\tau) - 1)(R(\tau) - 3),$$

$$H(0) = \frac{1}{R_0}, \quad J(\tau) = \frac{3}{R(\tau)} - 1.$$

For $\tau = 0$, P_2 is locally asymptotically stable whenever it exists since $H(0) > 0$. For $\tau > 0$, same as the discussion on $J(\tau)$ in the previous section, we define

$$\begin{aligned} I_- &= \{\tau \in (0, \tau_m) : J(\tau) < 0\} = (0, \tau_c), \\ I_+ &= \{\tau \in (0, \tau_m) : J(\tau) \geq 0\} = [\tau_c, \tau_m), \end{aligned} \tag{2.35}$$

where $\tau_c = \frac{1}{d_j} \log \frac{R_0}{3}$ is the unique root of $J(\tau)$.

Theorem 2.6: *If $R_0 \leq 3$, P_2 is locally asymptotically stable wherever it exists, i.e., $\tau \in [0, \tau_m)$.*

Proof. Since $R(\tau) = R_0 e^{-d_j \tau} < 3$, $\tau > 0$, thus $I_- = \emptyset$, $I_+ = [0, \tau_m)$, and stability does not change in I_+ . Notice that P_2 is stable when $\tau = 0$, therefore P_2 is stable for $\tau \in [0, \tau_m)$. \square

Global Hopf Branches and Multiple Stable Periodic Solutions

From bifurcation theories [Hale & Verduyn Lunel 1993], [Beretta & Kuang 2002], a pair of characteristic roots cross the imaginary axis to the right and a Hopf bifurcation starts at τ_{n1} , and when $\tau = \tau_{n2}$, a pair of characteristic roots cross the imaginary axis to the left and a Hopf bifurcation ends. From the previous study on a model with delay independent parameters, these start-values and

end-values may be connected by Hopf branches. To show the global behavior of these Hopf branches, we again employ the DDE-BIFTOOL. Here is the parameters used for simulation.

$$r = 1, \quad K = 50, \quad \beta = 0.08, \quad \gamma = 0.2, \quad d = 0.2, \quad d_j = 0.002 \quad (2.36)$$

Figure 2.12 is the graph for $S_n(\tau)$.

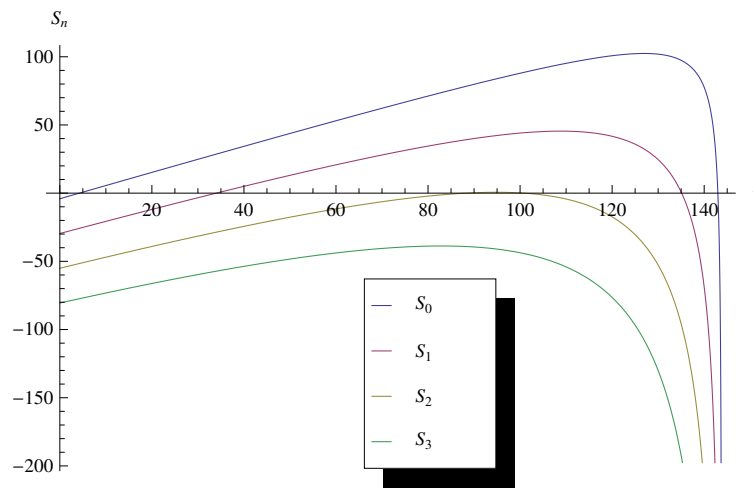


Figure 2.12: Graph of $S_n(\tau)$. We see that only S_0, S_1, S_2 have zeros.

Then we have

$$\begin{aligned} \text{on } S_0 : \quad & \tau_1^0 = 4.24465, \quad \tau_2^0 = 142.973; \\ \text{on } S_1 : \quad & \tau_1^1 = 33.9897, \quad \tau_2^1 = 135.109; \\ \text{on } S_2 : \quad & \tau_1^2 = 88.2029, \quad \tau_2^2 = 100.837. \end{aligned} \quad (2.37)$$

With the DDE-BIFTOOL, we come up with the global Hopf bifurcation graph, shown in Figure 2.13.

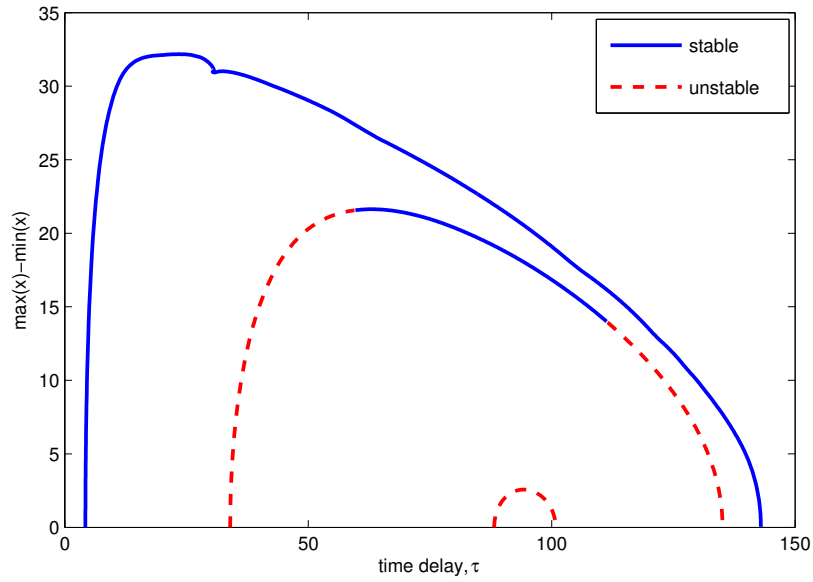


Figure 2.13: Global Hopf bifurcation.

We can see from Figure 2.13 that τ_1^n, τ_2^n are connected by a Hopf branch, similar as they are connected by $S_n(\tau)$, for $n = 0, 1, 2$. We also notice that there is an overlap of stable regions of the first two branches, which is then checked by DDE23 in MATLAB, as shown in Figure 2.14.

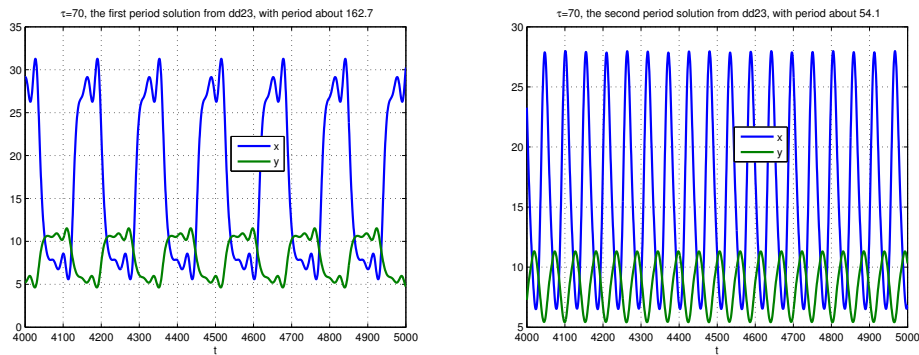


Figure 2.14: Two stable periodic solutions for $\tau = 70$, which lies in the overlap of the stable intervals in Figure 2.13.

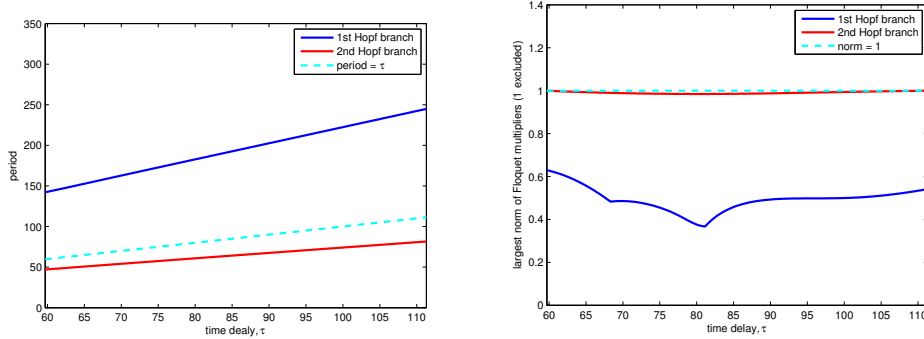


Figure 2.15: Left: periods of periodic solutions on the overlap stable region. Right: norm of the nontrivial Floquet multipliers with largest norm on the overlap stable region.

As one can see from the left graph in Figure 2.15, periodic solutions on the second Hopf branches oscillate faster (with smaller periods) and non-trivial Floquet multipliers are closer (and very close) to the unit cycle, which imply the stability of periodic solutions on the second branch are fragile and weaker than the ones on the first branch. Although the weaker periodic orbit is stable mathematically, some small perturbation about it may force the population to behave as the stronger periodic orbit as if it is unstable. As a consequence, it might be difficult to be observed in reality. It may also behave like a transient phenomenon.

2.D.5 Model with Holling Type II functional response: stability and global Hopf bifurcation

Assume $f(x) = \frac{x}{D+x}$, then coexistence equilibrium $P_2(x^*, y^*)$ is

$$x^* = \frac{D}{S-1}, \quad y^* = \frac{SD(S-D-1)}{(S-1)^2}, \quad (2.38)$$

where

$$S = \frac{\gamma}{d} e^{-d_j \tau},$$

and

$$R_0 = \frac{\gamma}{d} f(1) = \frac{\gamma}{d(1+D)}, \quad R(\tau) = R_0 e^{-d_j \tau} = \frac{S}{1+D}.$$

Existence of P_2 requires $R(\tau) > 1 \Leftrightarrow S > 1+D$, and if $R_0 > 1$, $\tau_m = \frac{1}{d_j} \log R_0$. We always assume $R_0 > 1$ (which also imply $\gamma > d$) as we will analyze P_2 only.

Other quantities are

$$H(0) = \frac{d(d(1+D) + \gamma(D-1))}{\gamma(\gamma-d)}, \quad (2.39)$$

$$\begin{aligned} J(\tau) &= \frac{d^2 e^{2d_j \tau} (1+D) + 2\gamma d D e^{d_j \tau} - \gamma^2}{\gamma(\gamma - d e^{d_j \tau})} \\ &= \frac{\left(\frac{d e^{d_j \tau}}{\gamma}\right)^2 (1+D) + 3D \left(\frac{d e^{d_j \tau}}{\gamma}\right) - 1}{1 - \left(\frac{d e^{d_j \tau}}{\gamma}\right)} \\ &= \frac{\left(\frac{1}{S}\right)^2 (1+D) + 3D \left(\frac{1}{S}\right) - 1}{1 - \left(\frac{1}{S}\right)}, \end{aligned} \quad (2.40)$$

As we discussed in the previous section, we know that stability of P_2 when $\tau = 0$ depends on $\text{sgn}\{H(0)\}$.

$$\begin{aligned} H(0) &> 0 \\ \Leftrightarrow d(1+D) + \gamma(D-1) &> 0 \\ \Leftrightarrow D &> \frac{\gamma-d}{\gamma+d} =: D_0, \end{aligned}$$

and

$$H(0) < 0 \iff D < \frac{\gamma - d}{\gamma + d} = D_0. \quad (2.41)$$

Thus if $D > D_0$, P_2 is locally asymptotic stable when $\tau = 0$, while if $D < D_0$, P_2 is unstable.

For $\tau > 0$, the same as we did previously, we need to determine $\text{sgn}\{J(\tau)\}$. Notice that the quantity $S = \frac{\gamma}{d}e^{-d_j\tau}$, since $\tau \in (0, \tau_m)$, plug this in and we get

$$(1 + D) < S < \frac{\gamma}{d} \iff \frac{d}{\gamma} < \frac{1}{S} < \frac{1}{1 + D}.$$

Let

$$h(s) = (1 + D)s^2 + 3Ds - 1.$$

One can see that $\text{sgn}\{J(\tau)\} = \text{sgn}\{h(1/S)\}$. It is obvious that $h(s)$ has exactly one positive solution, so does $J(\tau)$ since $1/S$ is a monotone function of τ . What we need to do next is to determine whether the unique positive $h(s)$ root lies in $(\frac{d}{\gamma}, \frac{1}{1+D})$. The sufficient and necessary condition for the positive root to be in $(\frac{d}{\gamma}, \frac{1}{1+D})$ is

$$0 > h(d/\gamma) \iff D < \frac{\gamma^2 - d^2}{d^2 + 3dr} =: D_1,$$

and

$$0 < h\left(\frac{1}{1+D}\right) \iff \frac{d}{\gamma} < \frac{1}{1+D}.$$

The second condition is satisfied always as $R_0 = \frac{\gamma}{d(1+D)} > 1$. Hence

$$J(\tau) \text{ has a positive root } \tau_c \text{ in } (0, \tau_m) \iff D < D_1,$$

where

$$\tau_c = \frac{1}{d_j} \log \frac{\gamma - 3D + \sqrt{9D^2 + 4(1+D)}}{2(1+D)}. \quad (2.42)$$

Noticing that $D_0 < D_1$, we have the following theorem.

Theorem 2.7: (i) If $D < D_0$, then P_2 is unstable when $\tau = 0$, $I_- = (0, \tau_c) \neq \emptyset$, $\omega(\tau)$ and $S_n(\tau)$ is unique and well defined in I_- .

(ii) If $D_0 < D < D_1$, then P_2 is stable when $\tau = 0$, $I_- = (0, \tau_c) \neq \emptyset$, $\omega(\tau)$ and $S_n(\tau)$ is unique and well defined in I_- .

(iii) If $D > D_1$, then P_2 is stable when $\tau = 0$ and $I_- = \emptyset$. Thus P_2 is stable for all $\tau \in (0, \tau_m)$.

Global Hopf Branches and Multiple Stable Periodic Solutions

Consider the following parameters:

$$r = 1, \quad K = 50, \quad D = 50, \quad b = 4, \quad \gamma = 0.2, \quad d = 0.2, \quad d_j = 0.001. \quad (2.43)$$

The we have $\tau_m = 693.15$, $\tau_c = 116.10$, and $H(0) > 0$. This is case (ii) in theorem 2.7.

Figure 2.16 is the graph for $S_n(\tau)$.

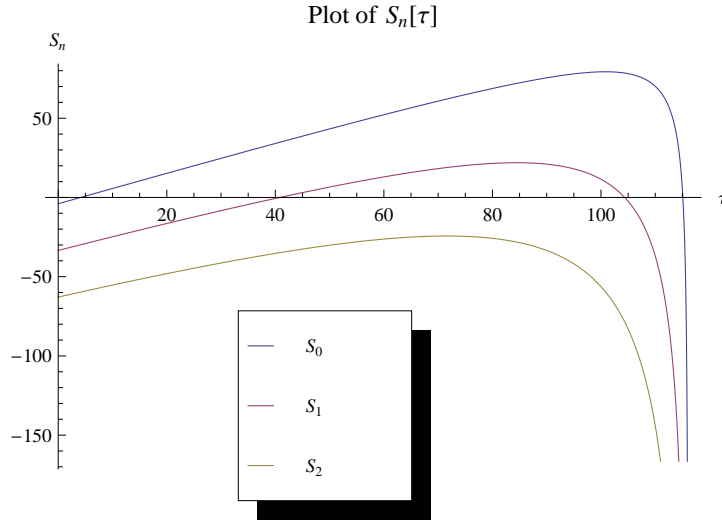


Figure 2.16: Graph of $S_n(\tau)$. We see that only S_0, S_1 have zeros.

Then we have

$$\begin{aligned}
 \text{on } S_0 : \quad \tau_1^0 &= 4.12, \quad \tau_2^0 = 115.08; \\
 \text{on } S_1 : \quad \tau_1^1 &= 40.83, \quad \tau_2^1 = 104.37.
 \end{aligned}
 \tag{2.44}$$

With the DDE-BIFTOOL, we come up with the global Hopf bifurcation graph, shown in Figure 2.13

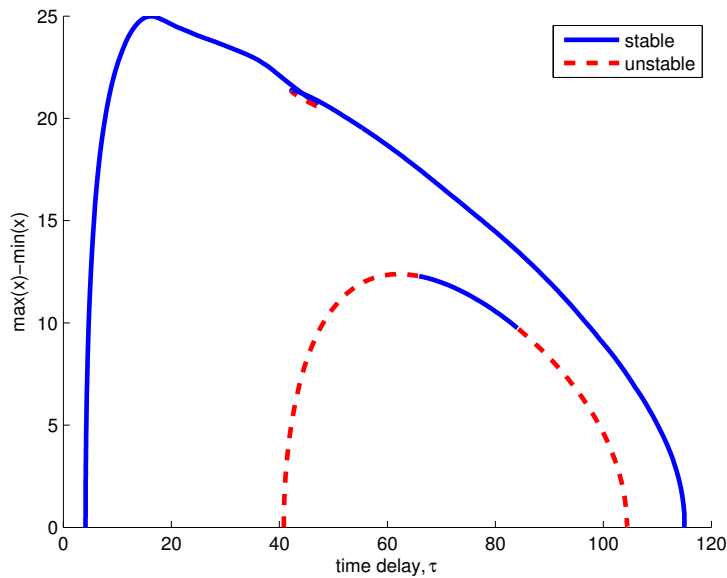


Figure 2.17: Global Hopf bifurcation.

We see again from Figure 2.17 that τ_1^n, τ_2^n are connected by a Hopf branch, similar as they are connected by $S_n(\tau)$, for $n = 0, 1$. We also notice that there is an overlap of stable regions of the first two branches, which is then checked by DDE23 in MATLAB, as shown in Figure 2.18. Furthermore, two torus bifurcations occur on the lower Hopf branch (Figure 2.19).

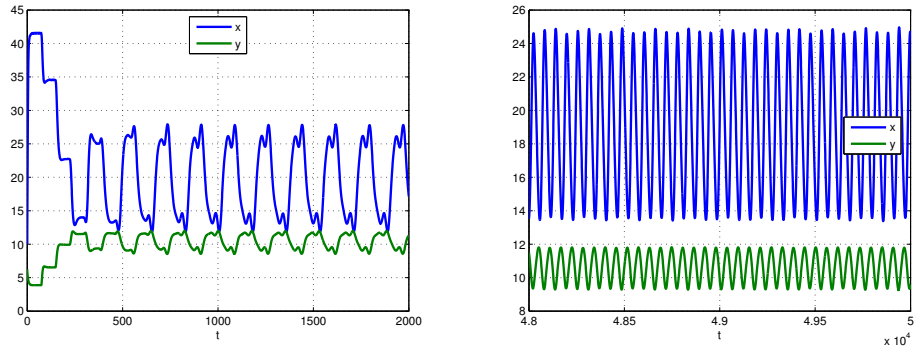


Figure 2.18: Two stable periodic solutions for $\tau = 73.5$, which lies in the overlap of the stable intervals in Figure 2.17.

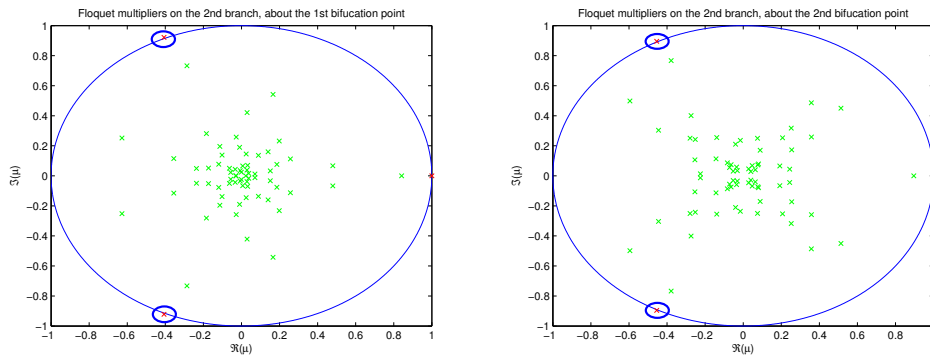


Figure 2.19: Torus bifurcations on the lower branch shown in 2.17 as a pair of complex Floquet multipliers cross the unit circle. Left: A pair of Floquet multipliers at the first secondary bifurcation point move inside the unit circle; Right: A pair of Floquet multipliers at the second secondary bifurcation point move outside the unit circle.

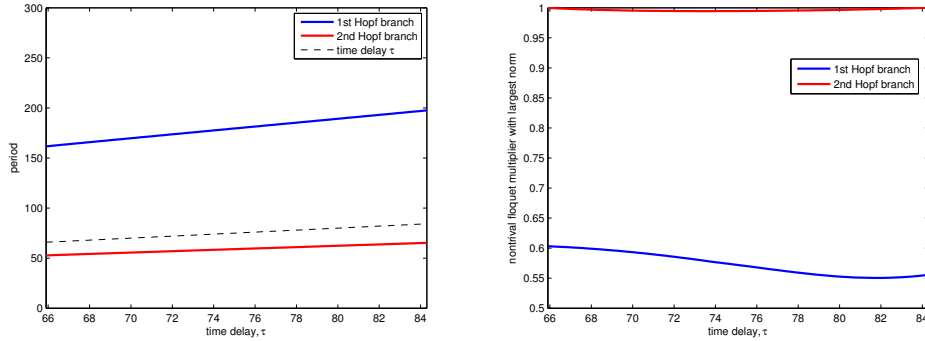


Figure 2.20: Left: periods of periodic solutions on the overlap stable region. Right: norm of the nontrivial Floquet multipliers with largest norm on the overlap stable region.

Again from the left graph in Figure 2.20, we see the same results as those in the model with Holling type I functionally response that periodic solutions on the second Hopf branches oscillate faster (with smaller periods) and non-trivial Floquet multipliers are closer (and very close) to the unit cycle.

2.D.6 Discussion

One can see that parameters we choose for simulations seem to be unreasonable as d_j which is referred to as the death rate of juveniles, should usually larger than the death rate of the adults. However, we think it is not always the case. If predators are those on top of a food chain, since juveniles who are

fed and protected by adults tend to be free or of lower risk from their fewer top predators, while adults who are out to hunt will have a large probability of being attacked by top predators, or may face the risk of being killed by the group effect of their preys while hunting them. Thus in this case, the d_j may be smaller than d . Indeed, numerical methods in DDE-BIFTOOL fails somewhere when plotting the first Hopf branch in the case that $d_j > d$. This in turn shows the limitation of the package. However, in the case that $d_j > d$, there still can be two or more $S_n(\tau)$ in Beretta and Kuang's Method intersecting with the τ -axis, which we think should also give the similar simple dynamics of the global Hopf branches as shown above.

If $d_j = 0$, then all the parameters are delay independent. Then the upper bound $\tau_m = +\infty$ and the unique positive root $\omega(\tau)$ of $F(\omega; \tau)$ is independent of τ , i.e. a constant, and so is $\theta(\tau)$. Therefore τ_n is the unique root of $S_n(\tau)$, and $S'_n(\tau_n) = 1$. From the previous study, we see that the interior equilibrium is unstable for $\tau > \tau_0$ if $R_0 > 3$. Thus models with delay independent parameters may overestimate the instability of interior equilibrium.

Chapter 3

Stability analysis of delay differential equations with two delays

In the real world, delays appear in almost every procedure, and models with only one delay are used under the assumption that other delays are small and insignificant to the systems. However, this assumption may not be applicable in cases when these delays are large and cause stability switches. For example, the predator prey model with delayed logistic growth and delayed maturation as follows:

$$\begin{aligned}x'(t) &= rx(t) \left(1 - \frac{x(t - \tau_1)}{K} \right) - \beta f(x(t))y(t), \\y'(t) &= \beta \gamma e^{-d_j \tau_2} f(x(t - \tau_2))y(t - \tau_2) - dy.\end{aligned}\tag{3.1}$$

As we know, without predators, the carrying capacity is a stable steady state for preys when $\tau_1 = 0$, while when τ_1 is large, the population of preys

will experience a periodic oscillation. Thus it is necessary to include this delay when τ_1 is large. Similarly, models with three or more delays may have to be considered in some cases.

Unfortunately, there is not an efficient way to analyze such a model at present, even with only two constant delays. The difficulty is to solve a quasipolynomial characteristic equation. In 2005, Gu et al develops a geometric method to find stability switching curves in models with two constant delays and delay-independent parameters, i.e., characteristic function of the form [Gu *et al.* 2005],

$$D(\lambda) = P_0(\lambda) + P_1(\lambda)e^{-\tau_1\lambda} + P_2(\lambda)e^{-\tau_2\lambda}, \quad (3.2)$$

where τ_1, τ_2 are the two delays, and

$$P_l(\lambda) = \sum_{k=0}^n p_{lk}\lambda^k.$$

This method is useful to analyze functional differential equations (both neutral and delayed types) with only one population and with delay independent parameters. For the system (3.1) even without the term $e^{-d_j\tau_2}$, Gu's method is not applicable.

In this chapter, we focus only on two-delay models. We first introduce our method to a more general characteristic function with delay-independent coefficients, and then look at cases with delay dependent parameters. These methods are still under developed and will be the future focus.

3.A Stability crossing curves of models with delay independent parameters

Consider characteristic equations of the form

$$D(\lambda) = P_0(\lambda) + P_1(\lambda)e^{-\lambda\tau_1} + P_2(\lambda)e^{-\lambda\tau_2} + P_3(\lambda)e^{-\lambda(\tau_1+\tau_2)}, \quad (3.3)$$

where τ_1, τ_2 are the two delays in R_+ , and

$$P_l(\lambda) = \sum_{k=0}^n p_{lk}\lambda^k.$$

The only difference to (3.2) is the appearance of the fourth term where the delays tangle together, and obviously if $P_3(\lambda) = 0$, (3.3) reduces to (3.2). Therefore, our analysis below is also applicable to (3.2).

To continue, at least we need to ensure that (3.3) is a characteristic equation of some DDE. Here are some basic assumptions.

(i) Finite solutions on $\mathbb{C}_+ := \{\lambda \in \mathbb{C} : \operatorname{Re}\lambda > 0\}$

$$\deg(P_0(\lambda)) \geq \max\{\deg(P_1(\lambda)), \deg(P_2(\lambda)), \deg(P_3(\lambda))\}. \quad (3.4)$$

(ii) Zero frequency

$\lambda = 0$ is not a characteristic root for any τ_1, τ_2 , i.e.,

$$P_0(0) + P_1(0) + P_2(0) + P_3(0) \neq 0.$$

(iii) The polynomials P_0, P_1, P_2, P_3 have no common zero, i.e., P_0, P_1, P_2, P_3

are coprime polynomials.

If (i) violates, then the characteristic equation can never be stable since there will be infinite number of roots with positive real parts [Bellman & Cooke 1963].

If (ii) is not satisfied, then $D(0, \tau_1, \tau_2) \equiv 0$ for all $(\tau_1, \tau_2) \in \mathbb{R}_+^2$, and therefore the characteristic function is always unstable.

Assumption (iii) is to ensure the characteristic equation considered has the lowest degree and is irreducible.

3.A.1 Stability crossing curves

Lemma 3.1: *As (τ_1, τ_2) varies continuously in \mathbb{R}_+^2 , the number of zeros (with multiplicity counted) of $D(\lambda; \tau_1, \tau_2)$ on \mathbb{C}_+ can change only if a zero appears on or cross the imaginary axis.*

This is just a direction inference of theorem (1.7) and Rouché theorem.

From this lemma, to study stability switch, we need to find the roots on the imaginary axis. Since $\lambda \neq 0$ by assumption (ii), and roots of a real function always come in conjugate pairs, we assume $\lambda = i\omega$ ($\omega > 0$). Plug this in and rewrite (3.3) as

$$D(i\omega; \tau_1, \tau_2) = (P_0(i\omega) + P_1(i\omega)e^{-i\omega\tau_1}) + (P_2(i\omega) + P_3(i\omega)e^{-i\omega\tau_1})e^{-i\omega\tau_2}. \quad (3.5)$$

Since $|e^{-i\omega\tau_2}| = 1$, we have

$$|P_0 + P_1 e^{-i\omega\tau_1}| = |P_2 + P_3 e^{-i\omega\tau_1}|, \quad (3.6)$$

which is equivalent to

$$(P_0 + P_1 e^{-i\omega\tau_1})(\bar{P}_0 + \bar{P}_1 e^{i\omega\tau_1}) = (P_2 + P_3 e^{-i\omega\tau_1})(\bar{P}_2 + \bar{P}_3 e^{i\omega\tau_1}).$$

After some simplification, we have

$$\begin{aligned} & |P_0|^2 + |P_1|^2 + 2\operatorname{Re}(P_0 \bar{P}_1) \cos(\omega\tau_1) - 2\operatorname{Im}(P_0 \bar{P}_1) \sin(\omega\tau_1) \\ &= |P_2|^2 + |P_3|^2 + 2\operatorname{Re}(P_2 \bar{P}_3) \cos(\omega\tau_1) - 2\operatorname{Im}(P_2 \bar{P}_3) \sin(\omega\tau_1). \end{aligned}$$

Thus,

$$|P_0|^2 + |P_1|^2 - |P_2|^2 - |P_3|^2 = 2A_1(\omega) \cos(\omega\tau_1) - 2B_1(\omega) \sin(\omega\tau_1), \quad (3.7)$$

where

$$\begin{aligned} A_1(\omega) &= \operatorname{Re}(P_2 \bar{P}_3) - \operatorname{Re}(P_0 \bar{P}_1), \\ B_1(\omega) &= \operatorname{Im}(P_2 \bar{P}_3) - \operatorname{Im}(P_0 \bar{P}_1). \end{aligned}$$

If there is some ω such that $A_1(\omega)^2 + B_1(\omega)^2 = 0$, then

$$A_1(\omega) = B_1(\omega) = 0 \iff P_0 \bar{P}_1 = P_2 \bar{P}_3. \quad (3.8)$$

Right hand of (3.7) is 0 with any τ_1 , and

$$|P_0|^2 + |P_1|^2 = |P_2|^2 + |P_3|^2. \quad (3.9)$$

Therefore, if there is an ω such that both (3.8) and (3.9) satisfied, then $\forall \tau_1 \in \mathbb{R}_+$ is a solution of (3.6).

If $A_1(\omega)^2 + B_1(\omega)^2 > 0$, then there exists an $\phi_1(\omega) \in [0, 2\pi)$ such that

$$A_1(\omega) = \sqrt{A_1(\omega)^2 + B_1(\omega)^2} \cos(\phi_1(\omega)),$$

$$B_1(\omega) = \sqrt{A_1(\omega)^2 + B_1(\omega)^2} \sin(\phi_1(\omega)).$$

Therefore, (3.7) becomes

$$|P_0|^2 + |P_1|^2 - |P_2|^2 - |P_3|^2 = 2\sqrt{A_1(\omega)^2 + B_1(\omega)^2} \cos(\phi_1(\omega) + \omega\tau_1). \quad (3.10)$$

Obviously, the sufficient and necessary condition for the existence of $\tau_1 \in \mathbb{R}_+$ satisfying the above equation is

$$||P_0|^2 + |P_1|^2 - |P_2|^2 - |P_3|^2| \leq 2\sqrt{A_1^2 + B_1^2}. \quad (3.11)$$

Denote Ω^1 to be $\omega \in \mathbb{R}_+$ satisfying (3.11). One should notice that (3.11) also includes the case when $A_1^2 + B_1^2 = 0$ (therefore (3.8), (3.9)).

Let

$$\cos(\psi_1(\omega)) = \frac{|P_0|^2 + |P_1|^2 - |P_2|^2 - |P_3|^2}{2\sqrt{A_1^2 + B_1^2}}, \quad \psi_1 \in [0, 2\pi),$$

We have

$$\tau_{1,n_1} = \frac{\psi_1(\omega) - \phi_1(\omega) + 2n_1\pi}{\omega}, \quad n_1 = -1, 0, 1, 2, \dots \quad (3.12)$$

All the formulas in these steps can be obtained explicitly. Once we get $\tau_1(\omega)$ given by (3.12), plug it into (3.5) and we get an explicit formula for $\tau_2(\omega)$ unconditionally with $\forall \omega \in \Omega^1$. Thus the stability crossing curves

$$\mathcal{T} := \{(\tau_1(\omega), \tau_2(\omega)) \in \mathbb{R}_+^2 : \omega \in \Omega^1\}. \quad (3.13)$$

Similarly, we can do the same analysis on τ_2 and get

$$\tau_{2,n_2} = \frac{\psi_2(\omega) - \phi_2(\omega) + 2n_2\pi}{\omega}, \quad n_2 = -1, 0, 1, 2, \dots, \quad (3.14)$$

where

$$\cos(\psi_2(\omega)) = \frac{|P_0|^2 - |P_1|^2 + |P_2|^2 - |P_3|^2}{2\sqrt{A_2^2 + B_2^2}}, \quad \psi_2 \in [0, 2\pi),$$

$$A_2(\omega) = \sqrt{A_2(\omega)^2 + B_2(\omega)^2} \cos(\phi_2(\omega)),$$

$$B_2(\omega) = \sqrt{A_2(\omega)^2 + B_2(\omega)^2} \sin(\phi_2(\omega)),$$

$$A_2(\omega) = \operatorname{Re}(P_1 \bar{P}_3) - \operatorname{Re}(P_0 \bar{P}_2),$$

$$B_2(\omega) = \operatorname{Im}(P_1 \bar{P}_3) - \operatorname{Im}(P_0 \bar{P}_2).$$

with the condition on ω to be

$$||P_0|^2 - |P_1|^2 + |P_2|^2 - |P_3|^2| \leq 2\sqrt{A_2^2 + B_2^2}. \quad (3.15)$$

which defines a region Ω^2 .

By squaring both sides of the two conditions (3.11) and (3.11), one can show that indeed

$$\Omega := \Omega^1 = \Omega^2.$$

We call Ω the crossing set. In fact, Ω consists a finite number of intervals of finite length, i.e.,

$$\Omega = \bigcup_{k=1}^N \Omega_k.$$

This is true because squares of both sides of (3.11) are polynomials, and any polynomial has a finite number of roots.

Plug $\tau_2(\omega)$ into (3.5) to get $\tau_1(\omega)$. It is obvious that the stability crossing curves obtained in this way should be the same as \mathcal{T} in (3.13). Since τ_1, τ_2 obtained in both ways depend only on $\omega \in \Omega$, therefore they should be the same respectively and can be defined as (3.12) and (3.14) as well to get the crossing curves, i.e.,

$$\mathcal{T} = \left\{ \left(\frac{\psi_1(\omega) - \phi_1(\omega) + 2n_1\pi}{\omega}, \frac{\psi_2(\omega) - \phi_2(\omega) + 2n_2\pi}{\omega} \right) \in \mathbb{R}_+^2 : \omega \in \Omega, \right. \\ \left. n_1, n_2 = -1, 0, 1, 2, \dots \right\}.$$

Since $\Omega = \bigcup_{k=1}^N \Omega_k$, we have

$$\mathcal{T} = \bigcup_{\substack{k=1,2,\dots,N \\ n_1=-1,0,1,\dots \\ n_2=-1,0,1,\dots}} \mathcal{T}_{n_1,n_2}^k, \quad (3.16)$$

$$\mathcal{T}_{n_1,n_2}^k = \{(\tau_1(\omega), \tau_2(\omega)) \in \mathbb{R}_+^2 : \omega \in \Omega_k\}. \quad (3.17)$$

One can show that each \mathcal{T}_{n_1,n_2}^k is continuous in \mathbb{R}_+^2 . In addition \mathcal{T}_{n_1,n_2}^k may connect with each other. Similar detail can be found in [Gu *et al.* 2005].

3.A.2 Crossing direction

Let $\lambda = \sigma + i\omega$. Then by the implicit function theorem, τ_1, τ_2 can be expressed as functions of σ and ω under some non-singular condition. For symbolic convenience, denote $\tau_3 := \tau_1 + \tau_2$.

$$R_0 := \left. \frac{\partial \operatorname{Re} D(\lambda; \tau_1, \tau_2)}{\partial \sigma} \right|_{\lambda=i\omega} = \operatorname{Re} \{ P'_0(i\omega) + \sum_{k=1}^3 (P'_k(i\omega) - \tau_k P_k(i\omega)) e^{-i\omega \tau_k} \}, \quad (3.18)$$

$$I_0 := \left. \frac{\partial \operatorname{Im} D(\lambda; \tau_1, \tau_2)}{\partial \sigma} \right|_{\lambda=i\omega} = \operatorname{Im} \{ P'_0(i\omega) + \sum_{k=1}^3 (P'_k(i\omega) - \tau_k P_k(i\omega)) e^{-i\omega \tau_k} \}. \quad (3.19)$$

Similarly, one can verify that

$$\left. \frac{\partial \operatorname{Re} D(\lambda; \tau_1, \tau_2)}{\partial \omega} \right|_{\lambda=i\omega} = -I_0, \quad (3.20)$$

$$\left. \frac{\partial \operatorname{Im} D(\lambda; \tau_1, \tau_2)}{\partial \omega} \right|_{\lambda=i\omega} = R_0. \quad (3.21)$$

We also have

$$R_l := \left. \frac{\partial \operatorname{Re} D(\lambda; \tau_1, \tau_2)}{\partial \tau_l} \right|_{\lambda=i\omega} = \operatorname{Re} \{ -i\omega (P_l(i\omega)e^{-i\omega\tau_l} + P_3(i\omega)e^{-i\omega(\tau_1+\tau_2)}) \}, \quad (3.22)$$

$$I_l := \left. \frac{\partial \operatorname{Im} D(\lambda; \tau_1, \tau_2)}{\partial \tau_l} \right|_{\lambda=i\omega} = \operatorname{Im} \{ -i\omega (P_l(i\omega)e^{-i\omega\tau_l} + P_3(i\omega)e^{-i\omega(\tau_1+\tau_2)}) \}, \quad (3.23)$$

where $l = 1, 2$.

By the implicit function theory, we have

$$\Delta(\omega) := \left(\begin{array}{cc} \frac{\partial \tau_1}{\partial \sigma} & \frac{\partial \tau_1}{\partial \omega} \\ \frac{\partial \tau_2}{\partial \sigma} & \frac{\partial \tau_2}{\partial \omega} \end{array} \right) \Bigg|_{\sigma=0, \omega \in \Omega} = \begin{pmatrix} R_1 & R_2 \\ I_1 & I_2 \end{pmatrix}^{-1} \begin{pmatrix} R_0 & -I_0 \\ I_0 & R_0 \end{pmatrix}. \quad (3.24)$$

The implicit function theorem applies as long as

$$\det \begin{pmatrix} R_1 & R_2 \\ I_1 & I_2 \end{pmatrix} = R_1 I_2 - R_2 I_1 \neq 0.$$

For any crossing curve \mathcal{T}_{n_1, n_2}^k . We call the direction of the curve corresponds to the increasing $\omega \in \Omega_k$ the *positive direction*, and the region on the left-hand (right-hand) side when we move in the positive direction of the curve *the region on the left (right)*. Since the tangent line of \mathcal{T}_{n_1, n_2}^k along the positive direction is $(\partial \tau_1 / \partial \omega, \partial \tau_2 / \partial \omega)$, the normal of \mathcal{T}_{n_1, n_2}^k pointing to the right region is $(\partial \tau_2 / \partial \omega, -\partial \tau_1 / \partial \omega)$. As we know, a pair of complex characteristic roots cross the imaginary axis to the right on the complex plane as σ increases

from negative to positive through 0, thus (τ_1, τ_2) moves along the direction $(\partial\tau_1/\partial\sigma, \partial\tau_2/\partial\sigma)$. As a consequence, we can conclude that if

$$\begin{aligned}\delta(\omega) &:= \left(\frac{\partial\tau_1}{\partial\sigma}, \frac{\partial\tau_2}{\partial\sigma}\right) \cdot \left(\frac{\partial\tau_2}{\partial\omega}, -\frac{\partial\tau_1}{\partial\omega}\right) \\ &= \frac{\partial\tau_1}{\partial\sigma} \frac{\partial\tau_2}{\partial\omega} - \frac{\partial\tau_2}{\partial\sigma} \frac{\partial\tau_1}{\partial\omega} \\ &= \det \Delta(\omega) > 0,\end{aligned}\tag{3.25}$$

the region on the left of \mathcal{T}_{n_1, n_2}^k has two more characteristic roots with positive real parts. On the other hand, if the inequality (3.25) is reversed, then region on the right has two more characteristic roots with positive real parts.

Since $\det \begin{pmatrix} R_0 & -I_0 \\ I_0 & R_0 \end{pmatrix} = R_0^2 + I_0^2 \geq 0$, we have

$$\text{sgn } \delta(\omega) = \text{sgn}\{R_1 I_2 - R_2 I_1\}.\tag{3.26}$$

If either $R_0 \neq 0$ or $I_0 \neq 0$. Furthermore, one can verify that

$$\begin{aligned}& R_1 I_2 - R_2 I_1 \\ &= \text{Im}\left\{-i\omega \overline{(P_1(i\omega)e^{-i\omega\tau_1} + P_3(i\omega)e^{-i\omega(\tau_1+\tau_2)})} i\omega (P_2(i\omega)e^{-i\omega\tau_2} + P_3(i\omega)e^{-i\omega(\tau_1+\tau_2)})\right\} \\ &= \omega^2 \text{Im}\{P_1(-i\omega)P_2(i\omega)e^{i\omega(\tau_1-\tau_2)} + P_1(-i\omega)P_3(i\omega)e^{-i\omega\tau_2} + P_2(i\omega)P_3(-i\omega)e^{i\omega\tau_1}\}.\end{aligned}\tag{3.27}$$

If we know the number of characteristic roots with positive real parts when $\tau_1 = \tau_2 = 0$, we can use the criterion (3.25) to find the number of characteristic roots with positive real parts for any (τ_1, τ_2) in \mathbb{R}_+^2 . Hence stability of the characteristic equation is completely known.

3.B Stability crossing curves of models with parameters depending on one delay

Consider characteristic equations of the form

$$D(\lambda; \tau, \tau_1) = P_0(\lambda; \tau) + P_1(\lambda; \tau)e^{-\lambda\tau} + P_2(\lambda; \tau)e^{-\lambda\tau_1} = 0, \quad (3.28)$$

where τ, τ_1 are the two delays in some interval I and \mathbb{R}_+ respectively, and

$$P_l(\lambda; \tau) = \sum_{k=0}^n p_{lk}(\tau)\lambda^k.$$

For convenience, we use P_l or $P_l(\lambda)$ to denote $P_l(\lambda; \tau)$, $l = 1, 2$. Similarly, we have the following assumptions.

(i) Finite solutions on the \mathbb{C}_+

$$\deg(P_0(\lambda)) > \max\{\deg(P_1(\lambda)), \deg(P_2(\lambda)), \deg(P_3(\lambda))\}. \quad (3.29)$$

(ii) Zero frequency

$\lambda = 0$ is not a characteristic root for any τ, τ_1 , i.e.,

$$P_0(0) + P_1(0) + P_2(0) + P_3(0) \neq 0.$$

We can play the some logic as the previous section and get

$$|P_0(i\omega; \tau) + P_1(i\omega; \tau)e^{-i\omega\tau}| = |P_2(i\omega; \tau)|, \quad (3.30)$$

from which we may expect to get a sequence of function $\tau(\omega)$ or $\omega(\tau)$ and then

plug it into (3.28) with $\lambda = i\omega$ ($\omega > 0$) to get τ_1 with no trouble.

Unfortunately, since ω and τ tangle in P_i , an explicit formula is impossible in general, and determining the domain of either $\tau(\omega)$ or $\omega(\tau)$ is impossible neither.

However, in some cases, we can use (3.30) to show that a model does not have stability switches when (3.30) contains no point (ω, τ) in $\mathbb{R}_+ \times I$, which can be easily plotted with MATLAB or other numerical programs. Furthermore, If for each $\omega > 0$ there is at most one solution τ in (3.30), or in the other way, then we can easily get an implicit function $\tau(\omega)$ or $\omega(\tau)$ numerically. Thus getting the stability crossing curves are much easier in the situation. In addition, stability crossing curves can also be detected in some cases with the DDE-BIFTOOL MATLAB package.

3.C An example: a population model with inner competition

Let x denote the adult population of some species, b and d to be per capita birth rate and death rate, then the simple population model including maturation delay is

$$x'(t) = be^{-d_j\tau}x(t - \tau) - dx(t). \quad (3.31)$$

Term $e^{-d_j\tau}$ is the probability a single juvenile grows to be an adult after the maturation period τ . d_j is the death rate of juveniles.

However, when considering the relation between individuals, we see that

there are competitions among them. Individuals compete for foods, space or any other resource. This type of competitions may have effects on the dynamics, and we should evaluate it. It is significant to notice that the effects of competitions on the population may not be seen immediately, thus we assume this delay to be τ_1 . Our model then becomes

$$\begin{aligned} x'(t) &= be^{-d_j\tau}x(t-\tau) - dx - lx^2(t-\tau_1) \\ &=: f(x(t), x(t-\tau), x(t-\tau_1)). \end{aligned} \tag{3.32}$$

Let $f(x, x, x) = 0$, and we get the two equilibria

$$x_0 = 0 \quad \text{and} \quad x^* = \frac{be^{-d_j\tau} - d}{l}.$$

For the equilibrium $x_0 = 0$, the correspondent linearized system is

$$x'(t) = be^{-d_j\tau}x(t-\tau) - dx(t),$$

which contains only one delay. Stability analysis is simple and will not be focused on in the following context.

For the positive equilibrium x^* , which required

$$b > d \quad \text{and} \quad \tau < \tau_m := \frac{1}{d_j} \log \frac{b}{d}.$$

The correspondent linearized system is

$$x'(t) = -dx + be^{-d_j\tau}x(t-\tau) - 2(be^{-d_j\tau} - d)x(t-\tau_1). \tag{3.33}$$

Assume (3.33) has solutions of the form $x = ce^{\lambda t}$, where $c > 0$ is a constant. Plug it into (3.33) and we get the characteristic equation

$$D(\lambda; \tau, \tau_1) = \lambda + d - be^{-d_j\tau}e^{-\lambda\tau} + 2(be^{-d_j\tau} - d)e^{-\lambda\tau_1} = 0. \quad (3.34)$$

For stability switch, we first look at case when $\tau = \tau_1 = 0$. In this case, there is only one characteristic root

$$\lambda = d - b < 0.$$

Thus x^* is stable when $\tau = \tau_1 = 0$.

To obtain stability switches, we consider pure imaginary roots $\lambda = i\omega$ ($\omega > 0$). Plug it into (3.34) and we get

$$i\omega + d - be^{-d_j\tau}e^{-i\omega\tau} = -2(be^{-d_j\tau} - d)e^{-i\omega\tau_1}. \quad (3.35)$$

Take the norm of both sides to get

$$\omega^2 + 2be^{-d_j\tau}\omega \sin(\omega\tau) - 2dbe^{-d_j\tau} \cos(\omega) + 8dbe^{-d_j\tau} - 3d^2 - 3b^2e^{-2d_j\tau} = 0. \quad (3.36)$$

We can see that separating the two variables is impossible. Instead, we choose to numerically find zero contours of the function on the left hand side (denoted as $g(\omega, \tau)$). For this purpose, we choose the following parameters and get Figure 3.1.

$$b = 0.5, \quad d = 0.1, \quad d_j = 0.3, \quad l = 0.01. \quad (3.37)$$

We see from Figure 3.1 that ω can be expressed implicitly as a function of

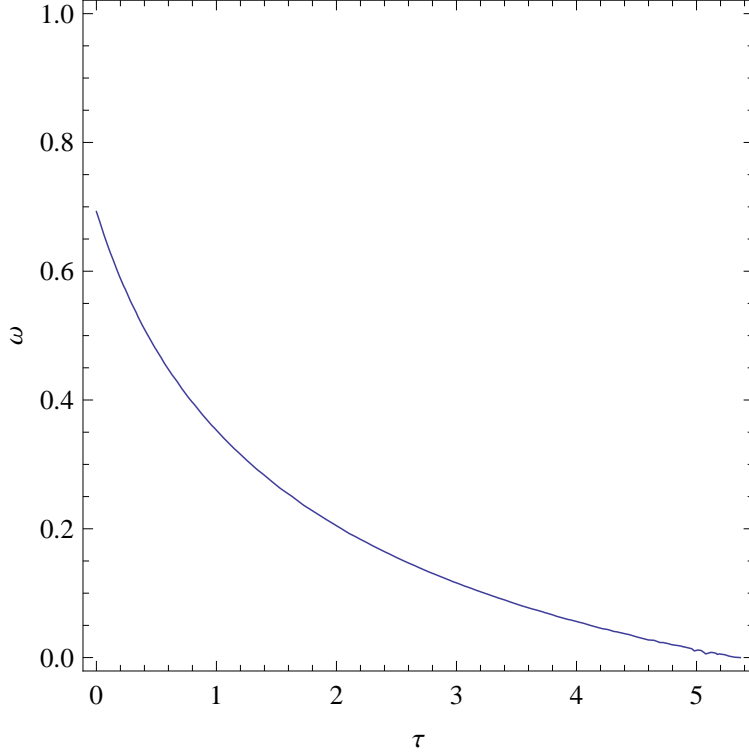


Figure 3.1: Zero contour of $g(\omega, \tau)$ with parameters given in (3.37), with which $\tau_m = 5.3648$.

τ . Plug it into (3.35) to get a sequence of $\tau_{1,n}(\tau)$ implicitly (Figure 3.2),

$$\tau_{1,n}(\tau) = \frac{1}{\omega(\tau)} \text{Arg} \left\{ \frac{2d - 2be^{-d_j\tau}}{i\omega(\tau) + d - be^{-d_j\tau}} \right\} + \frac{2n\pi}{\omega(\tau)}, \quad n = 0, 1, 2, \dots \quad (3.38)$$

In Figure (3.2), curves $\tau_{1,n}(\tau)$ separate the space $[0, \tau_m) \times \mathbb{R}_+$ into different connected regions, R_0, R_1, R_2, \dots , along the arrow. When (τ, τ_1) varies within a region R_n , the number of characteristic roots with positive real parts stays the same. It can change only when (τ, τ_1) crosses the curve $\tau_{1,n}(\tau)$ from R_n to R_{n+1} or R_{n-1} .

To obtain the number of characteristic roots with positive real parts and

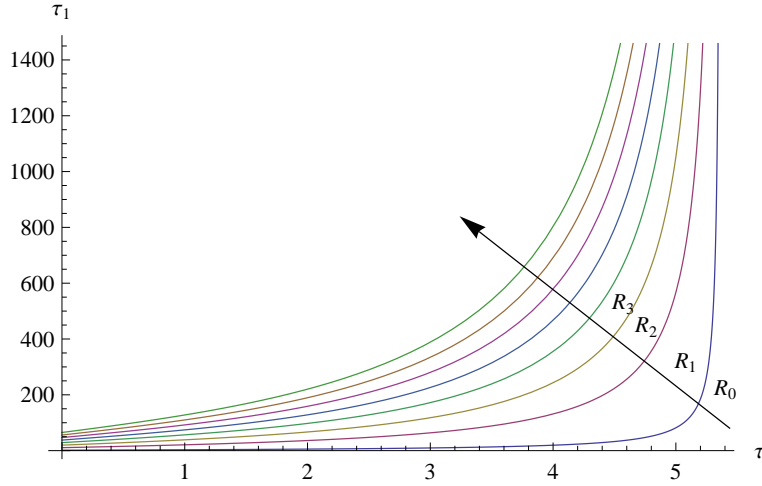


Figure 3.2: Stability crossing curves. The index n increases along the arrow.

determine local stability of x^* , we can analyze the case when $\tau = 0$ since every crossing curve has a unique intersection with the τ_1 axis at $\tau_{1,n}(0)$. From the study in chapter 2, we know that as τ_1 increases through $\tau_{1,n}(0)$, a pair of characteristic roots will cross the imaginary axis to the right on the complex plane. Since x^* is stable when $\tau = \tau_1 = 0$, there are $2n$ characteristic roots with positive real parts in region R_n , $n = 0, 1, 2, \dots$. The equilibrium x^* is asymptotically stable on R_0 and unstable in other regions.

Chapter 4

Discussion and future work

Through all the theories and examples shown in this thesis, we elucidate that introducing time delays to a dynamical system usually causes oscillations and instability. Small delays are harmless while large delays may completely change the dynamics. Therefore, ignoring delay in a process may lead to unreasonable results.

From the analysis in chapter 2, one can see dramatic differences between dynamics of models with delay independent parameters and models with delay dependent parameters, which seems to be a common rule. A scientist who constructs or applies a DDE model should keep this in mind, otherwise speculative or even erroneous statements may be deduced.

For DDEs with one delay, the method proposed by Beretta and Kuang is applicable to a large range of models. However, global behaviors of Hopf branches arising from critical delays are left to be further developed. The simple law shown in chapter 2 shows that all these critical delays are actually connected by Hopf branches, starting from where characteristic roots crossing the imaginary axis to the right and ending at where characteristic roots cross-

ing the imaginary axis to the left, or go unbounded. Multiple stable periodic solutions on these Hopf branches can occur. However, we do not know how common such a phenomenon is, and no proof has been presented. In addition, secondary bifurcations appearing on those branches also need theoretic support. These will be one main work in the future.

For models with delayed dependent parameters, examples here we show are cases that when $F(\omega)$ has only one positive root, thus only one S_n sequence. Simulations on cases when there are multiple S_n sequences, should be carried out in the future to see if all Hopf branches still connect critical τ values in the same way as S_n 's do. Or is there a cross connection, i.e., a Hopf branch connects two τ values from two different S_n 's, said S_n^1 and S_m^2 corresponding to two different positive roots of $F(\omega)$, ω_1 and ω_2 ?

Furthermore, theories and efficient numerical methods are needed for models with multiple delays, which are poorly studied at the present. Only models with two constant delays have been fully explored. From theories on models with one delay, one may expect that using a model with two delays and delay independent parameters as an approximation of a model with delay dependent parameters may lead to overestimate of instability. Any work on two-delay models with delay dependent parameters will be intriguingly and challenging but of great interest in many biological applications. This is another project we will carry out in the future.

Bibliography

- [Bangham 2000] C. Bangham, *Curr. Opin. Immunol.*, **12**:397, 2000.
- [Bellman & Cooke 1963] R. Bellman & K. Cooke, *Differential-Difference Equations*, Academic Press, New York, 1963.
- [Beretta & Kuang 2002] E. Beretta & Y. Kuang, *SIAM J. Math. Anal.*, **33**:1144, 2002.
- [Gu *et al.* 2005] K. Gu, S. Niculescu, & J. Chen, *J. Math. Anal. Appl.*, **311**:231, 2005.
- [Hale & Verduyn Lunel 1993] J. K. Hale & S. M. Verduyn Lunel, *Introduction to Functional Differential Equations*, New York: Springer-Verlag, 1993.
- [K. Engelborghs & Roose 2002] T. L. K. Engelborghs & D. Roose, *ACM Transactions on Mathematical Software*, **28**:1, 2002.
- [Kubota *et al.* 2000] R. Kubota, M. Osame, & S. Jacobson, *Effects of microbes on the immune system*, p. 349, 2000.
- [Li & Shu 2010a] M. Li & H. Shu, *Nonlinear Anal. Real World Appl.*, 2010.
- [Li & Shu 2010b] M. Li & H. Shu, *Bulletin of Mathematical Biology*, **73**:1774, 2010.
- [Osame *et al.* 1990] M. Osame, R. Janssen, H. Kubota, H. Nishitani, A. Igata, S. Nagataki, M. Mori, I. Goto, H. Shimabukuro, R. Khabbaz, & J. Kaplan, *Ann. Neurol.*, **28**:50, 1990.

- [Smith 2011] H. Smith, *An Introduction to Delay Differential Equations with Applications to the Life Sciences*, Springer, 2011.
- [Wang *et al.* 2007] K. Wang, W. Wang, H. Pang, & X. Liu, *Physica D*, **226**:197, 2007.
- [Wei & Li 2005] J. Wei & M. Li, *Nonlinear Analysis*, **60**:1351, 2005.
- [Wodarz & Bangham 2000] D. Wodarz & C. Bangham, *J. Mol. Evol.*, **50**:448, 2000.
- [Wu 1998] J. Wu, *Trans. Amer. Math. Soc.*, **350**:4799, 1998.